NAVAL POSTGRADUATE SCHOOL

MONTEREY, CALIFORNIA

THESIS

ANALYSIS OF THE ASSIGNMENT SCHEDULING CAPABILITY FOR UNMANNED AERIAL VEHICLES (ASC-U) SIMULATION TOOL

by

Christopher J. Nannini

June 2006

Thesis Advisor:	Arnold H. Buss
Thesis Co-Advisor:	Susan M. Sanchez
Second Reader:	Darryl K. Ahner

Approved for public release; distribution is unlimited

THIS PAGE INTENTIONALLY LEFT BLANK

REPORT DOCUMENTATION PAGE		*Form Approved OMB No. 0704-0188*

Public reporting burden for this collection of information is estimated to average 1 hour per response, including the time for reviewing instruction, searching existing data sources, gathering and maintaining the data needed, and completing and reviewing the collection of information. Send comments regarding this burden estimate or any other aspect of this collection of information, including suggestions for reducing this burden, to Washington headquarters Services, Directorate for Information Operations and Reports, 1215 Jefferson Davis Highway, Suite 1204, Arlington, VA 22202-4302, and to the Office of Management and Budget, Paperwork Reduction Project (0704-0188) Washington DC 20503.

1. AGENCY USE ONLY (*Leave blank*)	2. REPORT DATE June 2006	3. REPORT TYPE AND DATES COVERED Master's Thesis	
4. TITLE AND SUBTITLE: Analysis of the Assignment Scheduling Capability for Unmanned Aerial Vehicles (ASC-U) Simulation Tool		**5. FUNDING NUMBERS**	
6. AUTHOR(S) Christopher J. Nannini			

7. PERFORMING ORGANIZATION NAME(S) AND ADDRESS(ES)
    Naval Postgraduate School
    Monterey, CA 93943-5000
		8. PERFORMING ORGANIZATION REPORT NUMBER	

9. SPONSORING /MONITORING AGENCY NAME(S) AND ADDRESS(ES) N/A		**10. SPONSORING/MONITORING AGENCY REPORT NUMBER**	

11. SUPPLEMENTARY NOTES The views expressed in this thesis are those of the author and do not reflect the official policy or position of the Department of Defense or the U.S. Government.

12a. DISTRIBUTION / AVAILABILITY STATEMENT Approved for public release; distribution is unlimited	12b. DISTRIBUTION CODE

13. ABSTRACT (maximum 200 words)

        The U.S. Army Training and Doctrine Command (TRADOC) Analysis Center (TRAC) and the Modeling, Virtual Environments, and Simulations Institute (MOVES) at the Naval Postgraduate School, Monterey, California developed the Assignment Scheduling Capability for UAVs (ASC-U) simulation to assist in the analysis of unmanned aerial vehicle (UAV) requirements for the current and future force. ASC-U employs a discrete event simulation coupled with the optimization of a linear objective function. At regular intervals, ASC-U obtains an optimal solution to a simplified problem that assigns available UAVs to missions that are available or will be available within a future time horizon.

        This thesis simultaneously explores the effects of 26 simulation and UAV factors on the mission value derived when allocating UAVs to mission areas. The analysis assists in defining the near term (2008) UAV force structure and the investment strategy for the mid term (2013), and far term (2018). We combine an efficient experimental design, exploratory modeling, and data analysis to examine 514 variations of a scenario involving five UAV classes and over 21,000 mission areas. The conclusions suggest the following: the optimization interval significantly influences the quality of the solution, percent mission coverage may depend on a few UAV performance factors, small time horizons increase percent mission coverage, and carefully planned designs assist in the exploration of the outer and interior regions of the response surface.

14. SUBJECT TERMS Nearly Orthogonal Latin Hypercube, Design of Experiments, DOE, Multiple Regression Analysis, Simulation Analysis, Unmanned Aerial Vehicles, UAV, Discrete Event Simulation, SIMKIT, Future Combat Systems, FCS, Optimization			15. NUMBER OF PAGES 131
			16. PRICE CODE

17. SECURITY CLASSIFICATION OF REPORT Unclassified	18. SECURITY CLASSIFICATION OF THIS PAGE Unclassified	19. SECURITY CLASSIFICATION OF ABSTRACT Unclassified	20. LIMITATION OF ABSTRACT UL

THIS PAGE INTENTIONALLY LEFT BLANK

ANALYSIS OF THE ASSIGNMENT SCHEDULING CAPABILITY FOR UNMANNED AERIAL VEHICLES (ASC-U) SIMULATION TOOL

Christopher J. Nannini
Major, United States Army
B.S., Oregon State University, 1992
M.S., Oregon State University, 2002

Submitted in partial fulfillment of the
requirements for the degree of

MASTER OF SCIENCE IN OPERATIONS RESEARCH

from the

**NAVAL POSTGRADUATE SCHOOL
June 2006**

Author: Christopher J. Nannini

Approved by: Arnold H. Buss
                    Thesis Advisor

                    Susan M. Sanchez
                    Thesis Co-Advisor

                    Darryl K. Ahner
                    Second Reader

                    James N. Eagle
                    Chairman, Department of Operations Research

THIS PAGE INTENTIONALLY LEFT BLANK

ABSTRACT

The U.S. Army Training and Doctrine Command (TRADOC) Analysis Center (TRAC) and the Modeling, Virtual Environments, and Simulations Institute (MOVES) at the Naval Postgraduate School, Monterey, California, developed the Assignment Scheduling Capability for UAVs (ASC-U) simulation to assist in the analysis of unmanned aerial vehicle (UAV) requirements for the current and future force. ASC-U employs a discrete event simulation coupled with the optimization of a linear objective function. At regular intervals, ASC-U obtains an optimal solution to a simplified problem that assigns available UAVs to missions that are available or will be available within a future time horizon.

This thesis simultaneously explores the effects of 26 simulation and UAV factors on the mission value derived when allocating UAVs to mission areas. The analysis assists in defining the near term (2008) UAV force structure and the investment strategy for the mid term (2013), and far term (2018). We combine an efficient experimental design, exploratory modeling, and data analysis to examine 514 variations of a scenario involving five UAV classes and over 21,000 mission areas. The conclusions suggest the following: the optimization interval significantly influences the quality of the solution, percent mission coverage may depend on a few UAV performance factors, small time horizons increase percent mission coverage, and carefully planned designs assist in the exploration of the outer and interior regions of the response surface.

THIS PAGE INTENTIONALLY LEFT BLANK

TABLE OF CONTENTS

LIST OF FIGURES

LIST OF TABLES

THIS PAGE INTENTIONALLY LEFT BLANK

ACKNOWLEDGMENTS

THIS PAGE INTENTIONALLY LEFT BLANK

EXECUTIVE SUMMARY

The U.S. Army Training and Doctrine Command (TRADOC) Analysis Center (TRAC) and the Modeling, Virtual Environments, and Simulations Institute (MOVES) at the Naval Postgraduate School, Monterey, California developed the Assignment Scheduling Capability for UAVs (ASC-U) simulation tool to assist in the analysis of UAV requirements. TRAC selected ASC-U for the Army-wide UAV Mix Analysis that supports investment strategies involving technology for current operations, transitioning to modular forces, and developing and fielding the Future Combat Systems (FCS). The purpose of this thesis is to assess how changes in the input factors concerning simulation settings (time horizon and optimization interval) and UAV characteristics influence the Measures of Effectiveness (MOEs) generated by ASC-U.

This thesis explores the effects of 26 simulation and UAV factors on the MOEs generated by ASC-U. We focus on four specific areas of research concerning the allocation of UAVs within the ASC-U simulation:

1. What are the appropriate time horizons and optimization interval (decision point where UAVs are allocated to mission areas) to use within ASC-U?

2. Which UAV characteristics and performance capabilities significantly influence the MOEs?

3. Are there any significant interactions between factors or relationships between the MOEs?

4. What are appropriate Design of Experiment (DOE) methodologies and tools to incorporate into ASC-U for the Army's UAV Mix Analysis?

ASC-U is a scheduling model that applies UAV resources against the schedule of mission requirements within an operational scenario. ASC-U employs a discrete event simulation coupled with the optimization of a linear objective function. The model is based on the framework developed for Dynamic Allocation of Fires and Sensors used to evaluate factors associated with networking assets in the FCS. Given a scenario and a mix of UAVs, ASC-U determines a schedule for executing UAV missions. The

simulation tool considers airframe capabilities, payloads, the locations and capacities of ground control stations and launch and recovery sites, remote viewing terminals requirements, and communication footprints and.

The scenario consists of a set of mission area locations and requirements, friendly unit locations, platform and payload characteristics, and ground control characteristics. Each mission area has a set of sensor, weapon, or communication requirements. The mission areas do not move during the simulation. Rather, each area has a start and end time associated with it. As the simulation proceeds, mission areas "open" and "close" creating a time window in which UAVs with correct capabilities can service the mission. The number and type of UAVs constrain the solution, as do UAV performance capabilities such as air speed, operating time, transition time, and operating radius. The number and capacities of ground control stations (GCSs) and launch and recovery sites (LRSs) also constrain the solution. Additionally, the GCSs and LRSs move during the execution of the scenario.

The research conducted in this thesis takes advantage of experimental design techniques based on statistical theory and developed to assist researchers in the analysis of computer simulations. The primary goal of experimental design is to assess how changes in input parameters (factors) affect the results (responses). We select 26 factors for our exploration consisting of 25 UAV performance characteristics and the simulation's optimization interval. The ranges for the UAV factors are created by adding and subtracting 20% of the base scenario value. We set the range for the optimization interval between one and ten simulation hours.

We use the space-filling design of Nearly Orthogonal Latin Hypercubes (NOLH) to provide an exploration of the outer and interior regions of the response surface. NOLH designs allow the analyst to develop a comprehensive set of explanatory variables represented in the model. Instead of being restricted to two or three levels, the analyst can create a design that uses multiple or even a continuous range of values for each factor. This facilitates the identification of non-linearities within the response surface.

In addition to good space-filling properties, orthogonality is another feature of designs that make them effective. Orthogonal designs have no linear relationship between the regressors. The NOLH technique reduces the correlation between factor columns, creating a nearly orthogonal design matrix. We can examine the off-diagonal elements within the correlation matrix of the design in order to measure the level of orthogonality. The spreadsheet design tool used in the research has several features that guard against multicollinearity and produce a robust space-filling design.

We combine data analysis, exploratory modeling and a Nearly Orthogonal Latin Hypercube design to examine the output of 514 distinct scenarios (called design points). In doing so, we expand the use of ASC-U from running single scenarios with baseline settings to a full exploration across multiple factors. The application and insights gained will support current and future warfighters. Additionally, the research will assist in ASC-U's development and application across a robust set of future mission scenarios. The conclusions suggest the following:

- The optimization interval significantly influences the UAV schedule and its quality.

- Mission value and percent coverage are not equivalent MOEs.

- An optimization interval of one simulation hour provides better correlation between mission value and percent mission coverage.

- Longer time horizons result in poor allocation decisions, as observed in the coefficients of the regression models.

- Each measure of effectiveness has a different set of significant factors.

- Class I UAV operating time and Class IV operating radius are the main factors influencing 14 of 21 MOEs.

- Class IV UAV operating radius begins to make significant improvement to coverage at below baseline settings.

- Longer Class I UAV operating times increase all other UAV mission percent coverages.

- State-of-the-art design of experiment and data mining techniques yield insights impossible to gain otherwise.

THIS PAGE INTENTIONALLY LEFT BLANK

I.   INTRODUCTION

A.   BACKGROUND

During the past three years, the United States Army has developed three investment paths associated with equipping the Army. The paths include investments in the following: technology required for the immediate needs of current operations, transition to modular forces, and development and fielding of the Future Combat System (FCS) equipped forces. All of these investment paths include Unmanned Aerial Vehicles (UAVs), UAV organizations, UAV payloads, ground control capabilities, and sustainment (Witsken, 2004).

The Army's goal is to transition from the current modular force UAV mix to the future force UAV mix. The analysis supporting the evolution of the modular force will generate the key tasks and purpose that involve a future UAV capability, and recommend types and quantities of UAVs required by all types of maneuver and support brigades. (Witsken, 2004)   The Modeling, Virtual Environments, and Simulations Institute (MOVES) and the U.S. Army Training and Doctrine Command (TRADOC) Analysis Center (TRAC) at the Naval Postgraduate School developed the Assignment Scheduling Capability for UAVs (ASC-U) simulation tool to assist in the analysis of UAV requirements for the modular force.

ASC-U employs a discrete event simulation model coupled with the optimization of a linear objective function. ASC-U determines a schedule for UAV missions that can be successfully executed in a scenario with a specific mix of UAVs. At regular intervals, ASC-U obtains an optimal solution to a simplified problem that assigns available UAVs to missions that are available or will be available within a future time horizon.   The simulation derives an overall mission value for each assignment by considering the required flight time to each mission area and the amount of time each UAV covers the area.

The Director of TRAC wants to compare and correlate the methodology and results of ASC-U to other simulation programs such as Vector-In-Commander (VIC),

Advanced Warfighting Simulation (AWARS), Combined Arms and Support Task Force Evaluation Model (CASTFOREM), and Combat XXI. The objective is to assess the compatibility between all five models to ensure accurate UAV evaluation for future UAV studies (Witsken, 2004).

B.   PURPOSE

The purpose of this thesis is to assess how changes in the input factors concerning simulation settings (time horizon and optimization interval) and UAV characteristics influence the overall mission value and other MOEs derived when allocating UAVs to mission areas in the ASC-U simulation. Additionally, the analysis assists in defining the near term (2008) UAV force structure and the follow-on development of the investment strategy for the mid term (2013), and far term (2018) (Witsken, 2004).

C.   RESEARCH QUESTIONS

This thesis focuses on four specific areas of research concerning the allocation of UAVs within the ASC-U simulation:

1. What are the appropriate time horizons and optimization interval to use within ASC-U?

2. Which UAV characteristics and performance capabilities significantly influence the MOEs?

3. Are there any significant interactions between factors or relationships between the MOEs?

4. What are appropriate Design of Experiment (DOE) methodologies and tools to for the Army's UAV Mix Analysis?

D.   RESEARCH SCOPE

The Assignment Scheduling Capability for UAVs (ASC-U) simulation tool considers a dynamic UAV routing problem. It determines a feasible schedule for UAV missions given a scenario and a specific mix, type and number of UAVs. ASC-U does not consider several factors that may influence the solution, such as attrition of aircraft,

2

maintenance and sustainability, communications, terrain effects and weather. We do not consider these factors in this study. Our research is confined to investigating the factors considered by ASC-U that influence the allocation of UAVs to mission areas. The following areas provide the scope of our research:

- Define the capabilities of the simulation.
- Provide a DOE methodology for the simulation.
- Identify an appropriate optimization interval.
- Identify appropriate time horizons for UAV types.
- Assess the influence of factors on the MOEs supported by ASC-U.
- Conduct data analysis on the simulation output.
- Fit regression models to the data output.

## E.	THESIS ORGANIZATION

Chapter II introduces the Army's Future Combat System program. It provides an overview of the types of UAVs considered in the study. Included is a brief description of each aircraft and its capabilities. Chapter III discusses the formulation of the UAV allocation problem and describes ASC-U's approach to the solution. Chapter IV describes the selection of factors included in our experiment, the development of design points (scenarios) on which ASC-U is tested, and the statistical software selected for the analysis. Chapter V provides an analysis of the ASC-U output data and the regression models fit for 21 different MOEs. Chapter VI summarizes conclusions drawn from this overall study and provides recommendations for follow-on research.

THIS PAGE INTENTIONALLY LEFT BLANK

II.   FUTURE COMBAT SYSTEM

> It shall be a goal of the Armed Forces to achieve the fielding of unmanned, remotely controlled technology such that by 2010, one-third of the operational deep strike aircraft of the Armed Forces are unmanned; and by 2015, one-third of the operational ground combat vehicles of the Armed Forces are unmanned (106th Congress, 2000).
>
> National Defense Authorization Act for
> Fiscal Year 2001 H.R.4205, Sec. 217

The Army's Future Combat System (FCS) comprises a research, development, and acquisition program that extends over three decades and includes a multi-billion-dollar budget. The Chief of Staff of the Army (CSA) General Eric Shinseki introduced the FCS program in October 1999. The program originally entailed the transformation of the Army's Legacy Forces that is comprised of divisions into a lighter, modular organization called the Objective Force. Initial plans were to field the first of such modular-equipped forces in 2011 and complete the entire Objective Force by 2032. In order to bridge the gap between the Legacy Force and the Objective Force, and fill near-term warfighting requirements, the program called for an Interim Force consisting of active Army and Army National Guard units. These brigade-sized units are known as Interim Brigade Combat Teams (IBCTs) or Stryker Brigade Combat Teams (SBCTs). The first of such units have seen combat in Iraq. The last IBCT is scheduled for fielding in 2010 ("Unmanned Aircraft," 2005).

General Shinseki's successor, General Peter Schoomaker, changed portions of the FCS program in 2003. He started by redefining the Objective Force as the Future Force and called for spiral development, incorporating functional FCS capabilities as they became available. Additionally, General Schoomaker placed greater importance on the system of networks required to link Army forces as well as Joint forces together ("Unmanned Aircraft," 2005).

On July 21, 2004, the Army announced another round of restructuring for the FCS program. A primary objective of the restructuring included four phases of spiraling in new technologies to the existing force starting in fiscal year 2008. The remaining three spiral dates are scheduled to occur in 2010, 2012, and 2014. The second modular-equipped brigade, also known as a Unit of Action (UA), is scheduled for fielding in 2015 with two more brigades fielded each year after 2015 for a total of 15 FCS-equipped brigades ("Unmanned Aircraft," 2005).

The FCS is a joint networked *"system of systems."* The intent is to facilitate connectivity with other services, increase situational awareness, and allow for the synchronization of operations. The heart of the FCS relies on advanced technologies and an extensive communications network. Binding this network together are eighteen projected manned and unmanned systems. The net-centric dimension of the FCS is essential to the Future Force's capability to "*see first, understand first, act first, and finish decisively across the full spectrum of operations*" (Knarr, Haskins, & Mouras, 2001). Unmanned aerial vehicles are central to seeing and understanding the enemy first.

The ASC-U simulation tool is capable of modeling different scenarios with potentially unlimited varieties of UAVs. In this study, we consider several types of UAVs based on characteristics and performance capabilities of the Interim Force UAVs. These include the small (SUAV) and tactical (TUAV) vehicles, and the extended range multipurpose (ERMP) UAV. We also considered UAVs that will make up the modular brigades found in the Future Force. The following sections provide an overview of the different UAVs considered in the study. Included is a brief description of each aircraft and its capabilities.

A. SMALL UNMANNED AERIAL VEHICLE (SUAV)

Figure 1. SUAV – RQ-11 Raven (From "Raven UAVs," 2005).

In the 1990s, the Army became interested in UAVs capable of providing Reconnaissance, Surveillance and Target Acquisition (RSTA) at the company and platoon level. This capability requirement was reflected in the FCS program with the call for Class I and II UAVs beginning in 1999. The need for small unmanned aerial vehicles (SUAVs) increased as forces were deployed in Operation Enduring Freedom (OEF) in 2001 and again for Operation Iraqi Freedom (OIF) in 2003. Within 20 weeks of the authorization of program funding, the first of these lightweight vehicles were deployed with forces in OEF. Special Operations Forces and Rangers took advantage of the SUAVs in the rugged terrain of Afghanistan (Jenkins & Snodgrass, 2005). The Army purchased over 500 SUAVs for OEF and OIF ("Unmanned Aircraft," 2005). Commanders have been lauding their capabilities ever since.

What started this "rave" was a commercial off the shelf (COTS) device called the Raven, displayed in Figure 1. The RQ-11A Raven is considered a small unmanned aerial vehicle (SUAV). It provides intelligence, reconnaissance, and surveillance (ISR) capabilities to platoons through battalions in a variety of scenarios to include Military Operations in Urban Terrain (MOUT) (Jenkins & Snodgrass, 2005). AeroVironment Inc.

developed the Raven after its success with the FQM-151 Pointer that has deployed with the Marines, Army, and Air force since 1988 ("Unmanned Aircraft," 2005). Taking advantage of technology developments in batteries and microelectronics, the Raven is two-thirds the size and weight of its predecessor.

Table 1 displays the performance capabilities of the RQ-11B Raven. The Raven system consists of three airframes and one Ground Control Station (GCS). The platform runs on single-use and rechargeable batteries and is able to employ three sets of sensor packages: high-resolution day camera, high-resolution night imager, and a side-view thermal imager ("Unmanned Aerial," 2004). Crews hand-launch the Raven and recover it using an onboard autonomous pilot system (Jenkins & Snodgrass, 2005).

The Raven is a combat multiplier, providing units with beyond-line-of-sight (BLOS) capability and reduction of "troops to task" (TTT) by keeping soldiers out of harm's way when possible. The system transmits live video images, along with telemetry data such as compass headings and location, to ground control units (GCUs) and remote video terminals (RVTs) ("Unmanned Aircraft," 2005).

	RQ-11B		RQ-11B
Length	36 in	Wing Span	55 in
Gross Weight	4.0 lbs	Payload Weight	6.5 oz
Engine	direct drive electric	Battery	$LiSO_2$ Li-Ion
Endurance	90 min	Max Speeds	30 mph
Ceiling	1,000 ft	Operating Radius	10 km
Launch	hand	Landing	auto deep stall
Sensor	EO/IR		

Table 1.   Raven RQ-11B Characteristics and Performance Data (After "Unmanned Aircraft," 2005).

B.   TACTICAL UNMANNED AERIAL VEHICLE (TUAV)

Figure 2.   TUAV – RQ-7 Shadow (From "ERMP," 2005).

In December 1999, AAI Corporation, a subsidiary of United Industrial Corporation, was awarded an initial contract to produce a tactical unmanned aerial vehicle (TUAV) system. The system is designed to provide brigade commanders with a host of battle management capabilities to include target acquisition and battle damage assessment (BDA) ("U.S. Army," 2001). Thirty-three months later, the Assistant Secretary of the Army for Acquisition, Logistics and Technology, Claude Bolton Jr., authorized the Shadow 200 RQ-7 TUAV program to enter into full rate production. The contract with AAI Corporation is scheduled to provide 41 Shadow 200 TUAVs for the Army's six Stryker Brigade Combat Teams. All six brigades will receive the Shadow system by May 2006 (Mahnken, 2002). AAI's contract was a key success for the Army's Transformation program, demonstrating an accelerated effort to fill a capability gap for field commanders.

The Shadow, displayed in Figure 2, is intended for ground maneuver brigade commanders. It provides a sustainable capability for reconnaissance, surveillance, target acquisition and battle damage assessment. The aerial platform transmits images and telemetry data to control stations, providing the commander and his staff with valuable

information to plan, execute, and support ongoing missions. The TUAV's platoon consists of four airframes, six High Mobility Multi-purpose Wheeled Vehicles (HMMWV), two Ground Control Stations (GCS), four RVTs, antennas, and one Portable Ground Control Station (PGCS) and Data Terminal (PGDT) (Mahnken, 2002). The system includes three Shadow platforms with a fourth vehicle issued to the maintenance section ("AAI," 2006). The platoon consists of 22 personnel capable of sustaining flight operations on a 24-hour basis ("Unmanned Aerial," 2004).

Table 2 provides the performance capabilities of the RQ-7A Shadow. The TUAV has a wingspan of approximately 13 feet and has a gross weight of slightly over 300 pounds. It can carry a payload of 60 pounds and is equipped with an electro-optic/infrared sensor package. The platform is launched using a pneumatic launcher and is recovered using an automatic landing system. During flight, control of the Shadow can be transferred between GCUs; it can land at alternate LRSs to keep up with a brigade's rapid operational tempo (OPTEMPO) (Mahnken, 2002). The Shadow is capable of loitering above a mission area for four hours, at 50 kilometers from an LRS. It has a maximum range of 125 kilometers, operating at 8,000 to 10,000 feet during the day and 6,000 to 8,000 feet at night (Mahnken, 2002).

The Army's deputy chief of staff G-3 directed that the Shadow 2000 be fielded with every maneuver brigade in OIF and OEF. As of June 2004, Shadow platoons existed in five divisions and two Stryker brigades (2nd Infantry Division and 25th Infantry Division) ("Unmanned Aerial," 2004).

	RQ-7A	RQ-7B		RQ-7A	RQ-7B
Length	11.2 ft	11.2 ft	Wing Span	12.8 ft	14 ft
Gross Weight	327 lb	375 lb	Payload Capacity	60 lb	60 lb
Fuel Capacity	51 lb	73 lb	Fuel Type	MOGAS	MOGAS
Engine Make	UEL AR-741	UEL AR-741	Power	38 hp	38 hp
Data Link(s)	LOS C2 LOS Video	LOS C2 LOS Video	Frequency	S-band UHF C-band	S-band UHF C-band
Endurance	5 hr	7 hr	Max/Loiter Speeds	110/70 kt	105/60 kt
Ceiling	14,000 ft	15,000 ft	Operating Radius	68 nm	68 nm
Launch	catapult	catapult	Landing	arresting wire	arresting wire
Sensor	EO/IR	EO/IR	Sensor Make	Tamam POP 200	Tamam POP 300

Table 2.   Shadow RQ-7A/B Characteristics and Performance Data (After "Unmanned Aircraft," 2005).

C. EXTENDED RANGE MULTIPURPOSE (ERMP) UAV

Figure 3. ERMP – Warrior (From "ERMP," 2005).

The first endurance platform was the General Atomics RQ-1 Predator (Goebel, 2006). The "R" in the nomenclature indicates reconnaissance and the "Q" stands for the unmanned nature of the vehicle. The Predator first saw combat in Bosnia in 1995 and again in 1999 during Operation Allied Force (Kosovo). The UAV distinguished itself in ISR operations in Kosovo by providing video feeds to the command center at Aviano Airbase, Italy. Forward air controllers (FACs) used the information to acquire difficult targets. By the end of the conflict, the UAV was upgraded with laser designators (Bone & Bolkcom, 2003).

As the capabilities and sensor packages on the aircraft increased (strike and ISR), the nomenclature was changed to "M" for multi-mission (John, Shaver, Lynch, Amouzegar, & Snyder, 2005). With its new designation "MQ," the Predator was able to demonstrate its new capabilities starting in OEF (Bone & Bolkcom, 2003). The arched front of the aircraft contains a forward-looking Synthetic Aperture Radar (SAR) that scans from the "chin" panel. Westinghouse originally developed SAR for the cancelled US Navy A-12 strike aircraft. It provides 30-centimeter (1 foot) resolution at operational altitudes of 50,000 feet. The Versatron Skyball turret houses the electro-optic (EO) and infrared (IR) sensors (Goebel, 2006). The Predator is capable of carrying a laser

designator (LD) to illuminate targets in order to guide munitions launched by itself or other strike aircraft to their destination. The Predator uses direct radio frequencies (RF) or satellite links to receive and transmit control information and download data. The UAV provides real-time data to other platforms, such as the J-STARS surveillance aircraft, ground stations, and naval vessels (Goebel, 2006).

In the summer of 2005, the U.S. Army created an Extended Range Multi-Purpose (ERMP) UAV requirement. This initiative began with a contract to General Atomics for an enhanced Predator called the Warrior, displayed in Figure 3. The improved endurance aircraft will boast a heavy communication relay capability, enhanced strike payloads, and up to thirty-six hours of operating time (Bone & Bolkcom, 2003). Additional payloads include electro-optic/infrared (EO/IR) with laser designator and synthetic aperture radar/moving target indicator (SAR/MTI) ("Unmanned Aerial," 2004). The Army is planning to purchase 11 systems consisting of 12 UAVs and 5 control stations per system. The initial fielding is projected to begin in 2009 (Bone & Bolkcom, 2003). Table 3 provides the performance capabilities of the MQ-9A Predator.

	MQ-9A		MQ-9A
Length	36 ft	Wing Span	66 ft
Gross Weight	10,500 lb	Payload Capacity	*750 lb
Fuel Capacity	4,000 lb	Fuel Type	JP
Engine Make	Honeywell TPE 331-10	Power	900 shp
Data Link(s)	BLOS LOS	Frequency	Ku-band C-band
Endurance	30 hr clean/ 16-20 hr external stores	Max/Loiter Speeds	225/TBD kt
Ceiling	50,000 ft	Operating Radius	2,000 nm
Launch	runway	Landing	runway
Sensor	EO/IR	Sensor Make	MTS-B
	SAR/MTI	Weapons	4, 500 lb class or 8-10, 250 lb class
*Up to 3,000 lb total externally on wing hardpoints.			

Table 3. Predator MQ-9A Characteristics and Performance Data (After "Unmanned Aircraft," 2005).

D.   FUTURE COMBAT SYSTEM UAVS

The Army's concept of the FCS relies heavily on a communications network linking the system together. Unmanned vehicles are an integral component of the network and systems-of-systems assembly. The Army envisions unmanned aerial vehicles assigned to maneuver and support elements that include infantry, armor, scout, intelligence, aviation, artillery, and medical units. Mission capabilities include intelligence, surveillance and reconnaissance (ISR), battle damage assessment, targeting, convoy protection, chemical agent and improvised explosive device (IED) detection ("Unmanned Aerial," 2004). Integration and commonality across UAV systems will be essential for seamless and effective operations.

Each unit of action (UA) is projected to have approximately 200 UAVs that are organic across each echelon of the command from the platoon to brigade level (Erwin, 2003). The Army has defined four classes for the Future Force UAVs, based on the platform's capabilities and operational requirements ("Four FCS," 2005). The sizes and capabilities of the vehicles generally increase in subsequent classes. Platoons will operate Class I airframes. Companies and battalions will operate the Class II and Class III aircraft, respectively. Finally, brigades will operate the largest platform consisting of the Class IV UAV. The unmanned aircraft will carry out a variety of missions from communication relays to target acquisition capabilities. Table 4 provides the performance capabilities of the FCS UAVs.

	Class I UAV	Class II UAV	Class III UAV	Class IV UAV
Unit	Platoon	Company	Battalion	Brigade
Weight	5-10 lb	100-150 lb	300-500 lb	>3,000 lb
Endurance	50 min	2 hr	6 hr	6 hr
Radius	8 km	16 km	40 km	75 km
Transport	manpackable (35 lb system)	2 soldier remount	2 man lift	100 m x 50 m recovery area
Aircraft	Raven (interim)	TBD	Shadow (interim)	Fire Scout

Table 4.   FCS UAVs Characteristics and Performance Data (After "Unmanned Aircraft," 2005).

1.   Class I UAV
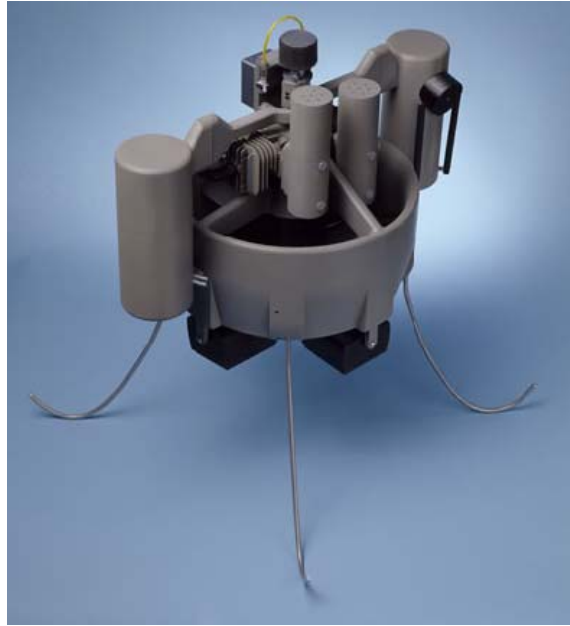
Figure 4.   Honeywell's Miniature Air Vehicle (From "Ducted Fan," 2005).

The Raven described in Section A provides the Interim Force with a Class I UAV capability at the battalion level. However, the Army plans to provide this capability down to platoon level. Honeywell Aerospace is moving towards this goal by developing the backpack-size Miniature Air Vehicle (MAV) displayed in Figure 4 ("Ducted Fan," 2005). In February 2006, Honeywell placed an order with AAI Corporation to produce 55 MAVs through November 2006. The platforms will be used in the Advanced Concept Technology Demonstration (ACTD) program of the Defense Advanced Research Projects Agency (DARPA) ("AAI," 2006). During the development phase, AAI will incorporate several new design features into the UAV.

The Class I vehicles have been coined with the term "hover and stare" due to their ability to take off and land like a helicopter and provide day or night video surveillance as well as still imagery. The design uses a ducted-fan technology that draws air in from the top and pushes it out from the bottom. The system is capable of flying along at 50 mph at an operational altitude of 100 to 500 feet above the ground and a maximum altitude of

over 10,000 feet. Current versions use gasoline and other heavy fuels common to U.S. Military ground vehicles and aircraft ("AAI," 2006).

Honeywell uses a flight management subsystem and micro-electrical mechanical systems (MEMS) to keep the device lightweight and provide autonomous flight features ("One Small," 2005). The 13-inch diameter, 17-pound modular system provides small units with reconnaissance capabilities that soldiers are able to carry in an infantryman's backpack ("AAI," 2006).

Another key reconnaissance feature of the platform is its "perch and stare" capability, when the MAV acts as an unattended ground sensor. While in this mode, the vehicle can provide video surveillance and conserve fuel at the same time. When the situation changes, the MAV can lift off and fly to another mission area (Crane, 2005).

2.   Class II UAV

Figure 5.   Class II – OAV II (From "Organic Air," 2005).

In July 2005, the Army's Future Combat Systems program entered into the first phase of development for the Class II UAV system. Serving as the Lead Systems Integrator (LSI) for the U.S. Army's FCS program, Boeing (along with Science Applications International Corporation (SAIC)) initiated a contract with Piasecki Aircraft

Corporation to develop its version of the Class II system called the Air Scout. Phase 1 is nearing its planned ten-month schedule, which has included an assessment of requirements and risk assessments of concepts for this class ("Four FCS," 2005). Up until this point, the FCS LSI and DARPA have been developing different technologies with the intent of narrowing down a final solution for the Class II UAV system. DARPA has focused on ducted fan technology resulting in the Organic Air Vehicle II (OAV II) displayed in Figure 5. Piasecki's platform, the Air Scout, uses a non-ducted fan system and resembles a smaller version of the PA-59H Airgeep II ("Four FCS," 2005).

By middle of 2006, selected LSI and DARPA platforms will be assessed for their ability to meet FCS capability requirements. This assessment will consist of a 24-month concept maturation phase. The phase will conclude with a flight assessment in 2008. At this point, the Class II UAV will enter a final System Design and Development (SDD) phase. The Army, LSI, and DARPA will use a cost-value comparison to select the FCS integrated UAV system. The first FCS system-of-systems testing will occur in 2010 with a projected follow-on fielding in 2014 ("Four FCS," 2005).

The Class II UAV is a unique system in that it will be vehicle mounted. This will enhance the platform's capability by allowing it to take off and land in unimproved areas as well as keeping its launch and recovery assets more mobile. Mobility will be critical since the UAV will provide reconnaissance, surveillance, and target acquisition for beyond-line-of-sight and non-line-of-sight engagements at the company level. The system will also boast autonomous control and man-in-the-loop cueing actions, freeing up soldiers to assess the enhanced imagery provided by the UAV ("Four FCS," 2005).

3. **Class III UAV**

Figure 6.   Class III – Prospector (From Latimer, 2005).

In October 2005, Teledyne Brown Engineering Inc., AAI Corp., and Piasecki Aircraft Corp. were awarded contracts for development on the Class III UAV system. The systems developed by these companies include the Prospector (Figure 6), Shadow III and the Air Guard, respectively ("Four FCS," 2005). The phases of development for this FCS platform are similar to the Class II UAV roadmap. Carried out in three phases, the process will involve the assessment of different technologies mounted on a variety of platforms. While DARPA chose a ducted fan technology for the OAV II, it selected a rotorcraft technology for its Class III version. LSI is investing in a gyrocopter and alternate fixed wing design for the system. A final candidate will be selected and ready for testing and fielding in 2010 and 2014 respectively ("Four FCS," 2005).

While some of the designs for the Class III resemble the Class II platforms, they are larger and have greater payload capacities. These UAVs will have extended endurance and be capable of carrying sensor packages suited for reconnaissance, communications relay, early warning, target acquisition and designation, and minefield detection to support battalion level operations ("Four FCS," 2005).

4. Class IV UAV

Figure 7.   Fire Scout RQ-8A (From "Fire Scout," 2004).

The Army selected the Fire Scout RQ-8B as its Class IV UAV in 2003. Northrop Grumman plans to deliver two prototypes in 2006 as part of an eight-year contract beginning in 2003 ("Unmanned Aircraft," 2005; "Fire Scout," 2004). Selection for the Class IV platform came more quickly than the other FCS UAVs due to the Fire Scout's successful developmental testing as the Fire Scout (RQ-8A) Vertical Take-Off and Landing (VTOL) Tactical UAV (VTUAV) program in the U.S. Navy ("Unmanned Aircraft," 2005). By 2005, the Fire Scout (Figure 7) had completed over 100 successful test flights incorporating Tactical Common Data Link (TCDL) operations, multiple sensor packages, and ground control systems ("Unmanned Aircraft," 2005).

Enhancements to the RQ-8B model include a four-blade rotor system versus the three-blade design on the RQ-8A, eight hours of operational time, and an increased payload weight of 600 pounds. The system also has an operational radius of 150 nautical miles ("Unmanned Aircraft," 2005; "Fire Scout," 2004). The four-blade rotor system allows the Fire Scout to carry several payloads at one time, increasing its operational capabilities at brigade level. This will allow brigade commanders to take advantage of the General Atomics Lynx Synthetic Aperture Radar with ground Moving Target

19

Indicator (SAR/MTI), an Electro-Optical/Infrared/Laser Designator range finder (EO/IR/LD), and a communication relay package simultaneously ("Fire Scout," 2004).

The Fire Scout will be able to support precision strike missions. The development program has resulted in the installation and testing of two four-packs of 2.75-inch rocket launchers designed to carry Advanced Precision Kill Weapon System laser-guided rockets and another laser-guided precision munition called Viper Strike ("Fire Scout," 2004). Table 5 provides the performance capabilities of the RQ-8B Fire Scout.

	RQ-8B		RQ-8B
Length	22.9 ft	Wing Span	27.5 ft
Gross Weight	3,150 lb	Payload Capacity	600 lb
Fuel Capacity	1,288 lb	Fuel Type	JP-5/JP-8
Engine Make	Rolls Royce 250-C20W	Power	420 shp
Data Link(s)	LOS C2 LOS Video	Frequency	Ku-band UHF C-band
Endurance	6+ hr	Max/Loiter Speed	125/0 kt
Ceiling	20,000 ft	Operating Radius	150 nm
Launch	vertical	Landing	hover
Sensor	EO/IR/LDRF	Sensor Make	FSI Brite Star II

Table 5.　　　Fire Scout RQ-8B Characteristics and Performance Data (After "Unmanned Aircraft," 2005).

E.　　　GROUND CONTROL AND MISSION PAYLOADS

Several controlling stations and devices make it feasible to launch, guide, and recover the unmanned vehicles. They also allow for the collection and evaluation of information provided by the various mission payloads on the platforms. This section provides a brief overview of the various ground control systems and mission payloads available for the UAVs described in this research.

1.　Launch and Recovery Site (LRS)

This thesis frequently refers to Launch and Recovery Sites versus a similar term, Launch and Recovery *Stations*. The former describes the geographic location where UAVs leave for and return from mission assignments. The latter refers to a mobile hardware component that assists flight control during the launch and recovery phases of the mission as the UAV takes-off and lands on the runway. From here on, we refer to Launch and Recovery Sites as LRSs unless otherwise stated.

ASC-U models the location of each LRS in the scenario with a grid coordinate system. During the length of the scenario, the location of an LRS may change depending on the mission requirement of its owning unit. LRSs vary in the type and number of UAVs that they can support. Once launched, flight control for the unmanned platform passes to a Ground Control Station (GCS).

2.　Ground Control Station (GCS)

Ground Control Stations house the electronic hardware to effectively command and control UAVs throughout the mission. The station usually consists of a rectangular shelter mounted on a vehicle such as the HMMWV displayed in Figure 8. The shelter contains pilot stations and monitors (Figure 9) in order to display video, still imagery, and sensor data provided by the mission payloads on the UAV.

Figure 8.   Ground Control Station (From Farmer, 2001).

While ASC-U is capable of modeling a wide range of GCS configurations, the simulation currently accounts for two types: the One System Ground Control Station (OSGCS), and the Dismounted Controller Device (DCD). The GCSs are unique in their capability to control different types of UAVs, and have a maximum capacity of platforms that they are able to handle at any given time.

AAI Corporation has produced the OSGCS for the Army's Shadow TUAV program since 2001. The system has logged over 50,000 hours during training and real-world operations. The One System GCS has controlled the Army Hunter platform, the Marine Corps' Pioneer TUAV system, and the Warrior UAV during demonstration flights in 2005. In October 2005, AAI Corp. was awarded a contract to produce the OSGCS system for the Warrior UAV.   Additionally, OSGCS meets NATO's standardization agreement (STANAG 4586), making it the control station of choice among allied military forces ("Army Orders," 2005).

Figure 9.   Ground Control Station Interior (From Farmer, 2001).

The Future Combat Systems LSI is investigating a multi-asset controller called the Dismounted Controller Device (DCD). The soldier carries and operates the device while on dismounted patrols or riding in vehicles. A key feature that currently separates the DCD from other control systems is its projected integration with the FCS family of systems. Along with UAVs, requirements call for the device to control several systems to include, but not limited to: Unmanned Ground Vehicles (UGVs), Manned Ground Vehicles (MGVs), Non-Line-of-Sight Launch Systems (NLOS-LS), Intelligent Munitions (IMS), and Unattended Ground Sensors (UGSs). The DCD will go through many interim fieldings as new technologies are developed. Human factors engineering will be essential to ensure that the device does not interfere with the soldiers' other mission-critical tasks ("FCS Dismounted," 2005).

3.   Remote Video Terminal (RVT)

The Remote Video Terminal (RVT) is a scaled down version of a GCS specifically designed to receive telemetry and video data directly from the UAV. The Army plans to field the terminals to command posts within battalions. Intelligence

analysts and fire support officers within Tactical Operation Centers (TOC) can download captured images with telemetry data for further analysis and execution of calls for fire.

A variant of the OSGCS called the One System Remote Video Terminal (OSRVT) is a mobile, manpackable terminal planned for the FCS family of systems. This device will feature an overlay containing icons for identified enemy units and vehicles in order to enhance target acquisition and identification ("Army Orders," 2005).

4.   Mission Payloads

Today's UAVs carry a variety of payloads that enhance their mission capabilities. ASC-U simulates UAVs with several different payloads depending on their type and intended missions.   While generating the solution, ASC-U matches mission areas requiring service by a payload or set of payloads with available UAVs capable of carrying the required payload. The mission payloads include:

- Electro-Optical/Infrared (EO/IR)
- Laser Rangefinder (LR)
- Laser Designator (LD)
- Synthetic Aperture Radar/Moving Target Indicator (SAR/MTI)
- Foliage Penetrating (FOPEN) Radar
- Light Detection and Ranging (LIDAR) Sensor Technology
- Electronic Warfare (EW)
- Global Positioning System (GPS) Designator
- Chemical, Biological, Radiological, Nuclear, Explosive (CBRNE)
- Weapon Systems
- Mine Detection
- Supply Delivery
- Communication Relay
- Meteorological Sensors
- Signals Intelligence (SIGINT)
- Communication Intelligence (COMINT)
- Electronic Intelligence (ELINT)

This chapter provided an overview of the different UAVs considered in the study. We also described several controlling stations and devices that make it feasible to launch, guide, and recover the unmanned vehicles. In the next chapter, we introduce ASC-U's approach to solving the dynamic routing problem involving UAVs.

THIS PAGE INTENTIONALLY LEFT BLANK

III. SIMULATION DESCRIPTION

A. UAV ALLOCATION PROBLEM

The U.S. Army Training and Doctrine Command (TRADOC) Analysis Center (TRAC) and the Modeling, Virtual Environments, and Simulations Institute (MOVES) at the Naval Postgraduate School, Monterey, California developed the Assignment Scheduling Capability for UAVs (ASC-U) simulation tool to assist in the analysis of UAV requirements for the current and future force. Figure 10 displays the study analysis process. The process has evolved within TRAC, separated into working groups responsible for components of this endeavor. Analysts link tactical scenarios with UAV mission requirements and performance capabilities. ASC-U uses the data to generate several measures of effectiveness (MOE) and a flight schedule for each scenario (Ahner, 2005b).

Each scenario provides a set of mission requirements. The screening tool uses UAV data to find feasible UAV mixes that satisfy mission requirements while meeting other goals.

Operational or Tactical Scenario

UAV Mission Requirements

UAV Data

Screening Tool

UAV Mix

Operating Environment
METT-TC Factors

UAV Missions
• Reconnaissance
• Target Acquisition
• Communications
• Sensor Payloads

Figure 10.   Study Analysis Process Diagram (After Ahner et al., 2006).

ASC-U is a scheduling model that applies UAV resources against the schedule of mission requirements, given the battlefield conditions within a scenario. ASC-U employs a discrete event simulation coupled with the optimization of a linear objective function.

The model is based on the framework developed by Havens (2002) for Dynamic Allocation of Fires and Sensors (DAFS) used to evaluate factors associated with networking assets in the Future Combat Systems. Given a scenario and a mix of UAVs, ASC-U determines a feasible schedule for UAV missions. The simulation tool considers airframe capabilities, payloads, the locations and capacities of ground control station and launch and recovery sites, remote viewing terminals requirements, and communication footprints and capacities (Ahner et al., 2006).

The scenario consists of a set of mission area locations and requirements, friendly unit locations, platform and payload characteristics, and ground control characteristics. Each mission area has a set of sensor, weapon, or communication requirements. The mission areas do not move during the simulation. Rather, each area has a start and end time associated with it. As the simulation proceeds, mission areas "open" and "close" creating a time window in which UAVs with correct capabilities can service the mission. The number and type of UAVs constrain the solution, as do UAV performance capabilities such as air speed, operating time, transition time, and operating radius. The number and capacities of ground control stations (GCSs) and launch and recovery sites (LRSs) also constrain the solution. Additionally, the GCSs and LRSs move during the execution of the scenario (Ahner et al., 2006).

ASC-U employs a Discrete Event Simulation (DES) model that simulates the operational environment of the UAVs. The simulation is based on Simkit developed by Professor Arnold Buss at the Modeling, Virtual Environments, and Simulations Institute (MOVES) at the Naval Postgraduate School, Monterey, California. Simkit is written in Java 2™ and is free to download at the Simkit website (Buss, 2006). The simulation component within ASC-U accounts for the geographical dispersion of UAVs, ground control systems, and mission areas within the scenario. The DES model simulates travel, loiter, and transition times. The flight schedule takes into account the actual routing of UAVs over time and distance and results in a realistic and feasible product for each scenario.

ASC-U blends optimization and simulation techniques to solve the complex assignment and scheduling problem presented by the scenarios in the Army's UAV Mix

Analysis. It handles the UAV routing problem with a "rolling algorithm." This results in an optimal assignment of each available UAV to at most one mission area during the specified time horizon at every optimization step. This problem is simpler than the general UAV scheduling problem because at any given point in time it restricts the set of missions that will be considered, as well as the number of missions that can be assigned to a specific UAV. While ASC-U is not guaranteed to provide an optimal solution, the "rolling algorithm" provides a systematic method of obtaining "good" schedules with a reasonable amount of computing effort. The impacts of the time horizon and the optimization interval on solution quality are evaluated as part of this study.

B.   DYNAMIC PROGRAMMING APPROACH

ASC-U uses an approximate dynamic programming approach known as a "rolling horizon" approach. This method accounts for state transitions within the simulation rather than modeling them in an optimization formulation. The approach is able to spiral in new problem characteristics such as UAV attrition and enable many measures of effectiveness to be collected and reported (Ahner, 2005b).

ASC-U   obtains   an   optimal   solution to   a   simplified   problem by assigning each available UAV to at most one mission that is currently available or will be available within a future time horizon. The time horizon is unique to each type of UAV. The simulation derives a mission value for each assignment by considering the amount of time each UAV is on-station at a mission area and a value rate for sensor requirement within a mission area. The time horizon is used to identify the missions that become available and does not influence the value of the service time. The simulation schedules UAVs to leave LRSs and arrive at mission areas in time to achieve the maximum value for servicing the area. The process advances to the next optimization interval and assesses all UAVs not yet launched even if they were scheduled to launch in the previous optimization period. Available UAVs are assigned to missions that do not yet have a UAV scheduled to that mission (Ahner, 2005a).

Figure 11 displays the dynamic process of assigning two UAVs to five mission areas. The optimization interval for the scenario is set at t simulation hours. The arrows

at point 1 indicate the first (t_0) and second (t_1) optimization periods. At time t_0, two UAVs are available, UAV 1 and UAV 2. ASC-U assesses available UAVs with GCS resources and available missions within the time horizon spanning t_0 to t_2. Within this time horizon, missions 1, 2, and 3 are considered. At point 2, the UAVs with appropriate sensor payloads are assigned to mission areas requiring service by such a payload. For our example, assume that it is best to assign UAV 1 and UAV 2 to missions 1 and 2, respectively. The simulation schedules UAV 1 to launch immediately, accounts for its flight time, and schedules its arrival at mission 1 as indicated by point 3. Notice that UAV 2 is scheduled to launch shortly after t_1 in order to arrive just in time to begin service at mission 2. At each optimization interval, ASC-U considers all available UAVs, this includes aircraft that are scheduled but not launched. At time t_1, UAV 2 is scheduled but not launched, and is therefore "unassigned" and considered as an available UAV for the second optimization period as indicated at point 4. Now, the time horizon includes missions 1, 2, 3, and 4. UAV 2 achieves a higher assignment value for serving mission 4 then it did for mission 2 and reschedules to launch at point 5. The simulation does not reassign UAVs while in flight. In this manner, the simulation builds a flight schedule based on the optimal assignments achieved within the fixed time horizons (Ahner et al., 2006).
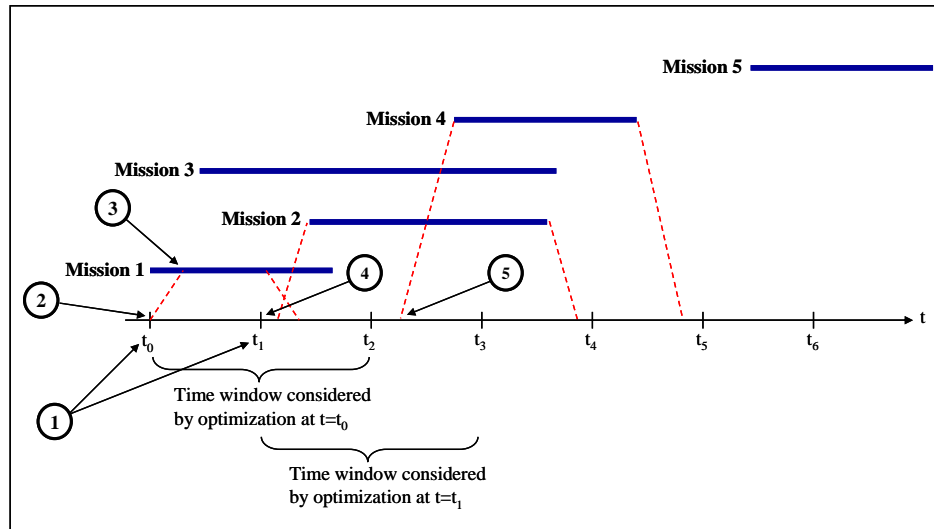
Figure 11.   Assignment Dynamics Example (After Ahner et al., 2006).

30

The simulation determines the mission value for flying a UAV to each mission using a valuation rate for sensor requirements on each mission area. The sensor valuation rates depend on user-input. This gives ASC-U the flexibility of use as an analytical tool for UAV mix studies as well as by operational commands that wish to prescribe priorities to different missions. The UAV's time-on-station for available missions is multiplied by the value rate in order to calculate the mission value for each UAV-mission pairing (Ahner et al., 2006).

Figure 12 displays the dynamic cueing and transition process conducted by ASC-U in order to build the UAV flight schedule. The Dynamic Simulation State Transition indicates the state of the system immediately prior to the next optimization interval. For discussion, let the simulation state exist at time zero. Airframes are located with their respective LRSs and dispersed according to the scenario's initial battlespace configuration. The simulation triggers its first optimization interval as we saw in Figure 11. The optimization sequence employs the Value of Potential Assignment Generator to calculate the value for all possible UAV-mission pairings that occur within the time horizons of each UAV by type. The Generator considers movement, ranges, and capacities of the ground control systems and passes the data along with the mission values to the Optimization. The Optimization makes assignments based on the maximum value obtained for each UAV-mission pairing and sends the results to the UAV Scheduler. The UAV Scheduler determines launch times for assigned UAVs resulting in a flight schedule that accounts for travel and service times for each mission area. The simulation proceeds to execute all ingress and egress flights as well as payload/sensor actions on assigned mission areas that occur before the next optimization interval. This continues until the completion of the scenario (Ahner et al., 2006).

The value of each assignment is determined BEFORE the optimization taking into account travel time, time-on-station, LRS location over time, and GCS location and capacity over time.

Values of assignments are passed to Optimization.

Value of Potential Assignment Generator

Optimization

Optimization provides "optimal" assignment as cues for where airframes should go.

Periodic or event triggered reoptimization

Dynamic Simulation State Transitions

UAV Scheduler

The UAV Scheduler determines when airframes should be launched to locations given to it by the optimization.

Figure 12.   ASC-U Dynamic Cueing and Transitions (After Ahner et al., 2006).

This thesis investigated a scenario involving 21,360 mission areas. The parameters for the mission areas are represented in a Microsoft® Excel® spreadsheet and loaded into ASC-U prior to each simulation run. Currently, mission areas implemented in ASC-U capture the following details: Cartesian coordinates for location; start and end times; mission package requirements; value rate for allocating UAV assets; and Army Universal Task List (AUTL) tasks associated with each mission. Figure 13 displays a Cartesian coordinate plot of the mission areas and ground control systems. We note that TRAC developed several larger scenarios (which consist of over 40,000 mission areas) during and after the data analysis phase of this thesis. We were not able to explore the additional scenarios within this thesis due to the unavailability of data.
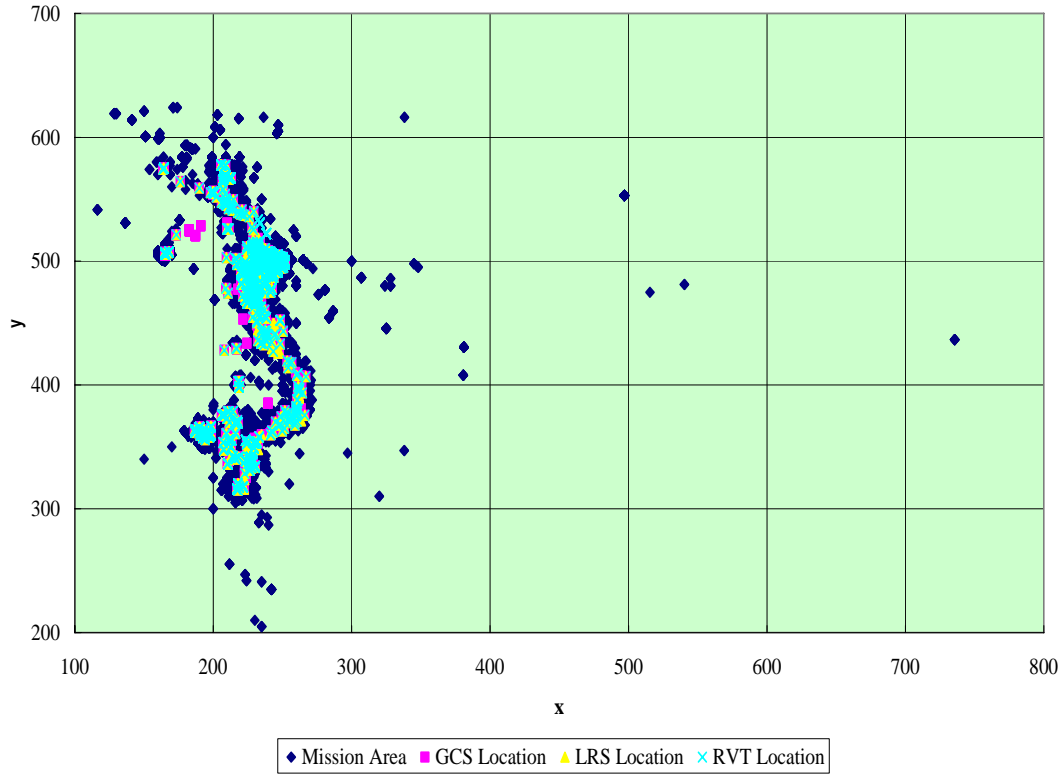
Figure 13.   Cartesian Coordinate Plot of Mission Areas and Ground Control Systems.

C.   CONSTRAINTS, LIMITATIONS, AND ASSUMPTIONS

This section describes the constraints, limitations, and assumptions made by the developers of ASC-U. Constraints represent uncontrollable conditions that influenced the development of the simulation. Limitations represent conditions that the developers defined to scope the solution. Assumptions represent choices made by the developers to simplify the problem into a manageable set of components in order to generate a solution (Ahner et al., 2006).

1.   Constraints

Two conditions acted as constraints during the development of ASC-U, problem type and time. The problem type is a combination of vehicle assignment and routing problems. Similar problems have been identified as "NP-hard" and hinder analysts' ability to generate a solution in a polynomial number of computational steps (Ahner et

al., 2006). The difficulty lies in the process of enumerating all of the UAV-mission assignments in order to develop the optimal schedule within a reasonable amount of time.

The developers were also limited by time available to construct a tool required for the Army's UAV Mix Analysis. Once developed, however, ASC-U leveraged the ability to incorporate additional capabilities and enhancements. The simulation is able to spiral in new problem characteristics and maintain flexibility in future studies (Ahner et al., 2006).

2. Limitations

The following is a list of limitations from the ASC-U Users/Analyst Manual (Ahner et al., 2006):

- ASC-U represents mission areas as a single Cartesian coordinate for the entire mission window. If more than one UAV is required to perform a mission, the user must provide sensor requirements at two different/adjacent coordinates. The use of single coordinates for mission areas account for the first order effects of assignments over space and time and GCS capacity and range constraints.

- ASC-U does not account for tactics, techniques, and procedures concerning the employment of UAVs as they serve mission areas.

- The UAV remains at the mission area until all sensor requirements that the UAV can perform end or the UAV must return to its LRS so that it does not exceed its operating time.

- ASC-U does not model passing UAV control between two GCSs. A single GCS controls a UAV throughout its entire mission.

- The user defines the contents of a sensor package for each UAV type prior to running the simulation. Sensor packages cannot be reconfigured during the simulation.

- The user provides LRS and GCS locations for particular times throughout the length of the scenario. LRSs and GCSs travel at a uniform rate between the locations during the prescribed times.

3. Assumptions

The following is a list of assumptions from the ASC-U Users/Analyst Manual. The authors note that some limitations may be considered as assumptions in order to highlight their effect on the solution (Ahner et al., 2006).

- The overall mission value for the scenario is the sum of the sensor requirement values for served mission areas making up the solution.

- UAV airspeed and operating radius are constant.

- UAV control and data link requirements are satisfied.

- Transition times between flights are constant.

- Transition times represent recovery of UAVs and include swapping payloads.

- The simulation does not consider attrition of or damage to UAVs. Additionally, maintenance requirements are not considered.

- Army Airspace Command and Control (A2C2) requirements are satisfied.

- The locations of the GCSs and LRSs locations are extracted from a Map Exercise (MAPEX) or a simulation running an approved scenario and are known throughout the scenario.

- LRSs and GCSs travel at a uniform rate between locations from start to end times.

- GCSs often operate in pairs, employing a "leap frog" movement where one controls UAVs from a forward position while the other GCS moves to its next position. ASC-U replicates this method of employment by representing two GCSs by a single GCS that operates continuously with uniform movement between positions. This modeling technique allows for uninterrupted GCS capacity and control between positions.

- LRSs are within range of at least one GCS for launch and recovery operations.

- Terrain features do not influence UAV mission accomplishment. ASC-U does not model terrain features within the simulation.

- Atmospheric conditions do not influence UAV mission accomplishment. ASC-U does not model atmospheric conditions within the simulation.

D.   ASC-U INPUT

The mission requirements and UAV performance characteristics are represented in a Microsoft® Excel® spreadsheet. The user/analyst loads the spreadsheet into ASC-U prior to each simulation run. The Excel® file has several worksheets, each provide data for a specific component of the mission requirements. Table 6 displays the name of the worksheets included in the Excel® input file.

Our research explored the effects of twenty-six simulation and UAV performance factors on the mission value derived when allocating UAVs to mission areas. The factors consisted of the following: optimization interval, time horizons, air speed, operating time, operating radius, and transition time. While the optimization interval is a single value for the entire scenario, the other five factors are unique for each type of UAV. The MetaData worksheet stores the optimization interval and the AirFrame worksheet lists the UAV performance factors. The following sections provide a description of the worksheet components used for the research conducted in this thesis. For a complete description of the input worksheets used by ASC-U, see the current version of the ASC-U Users/Analyst Manual (Ahner et al., 2006).

Worksheet Title
MetaData
Mission
AirFrame
MissionPackageTypes
MissionPackageLocation
GCSInput
LRSInput
RVTInput
SuperMissionData

Table 6.   ASC-U Input Worksheets (From Ahner et al., 2006).

1. Meta Data Worksheet

The MetaData worksheet contains three elements: scenario length, optimization interval, and report interval (Ahner et al., 2006). We investigated the optimization interval in this thesis.

- **Scenario length** indicates the length of the scenario in simulation hours. (Defaults to 360.0, if MetaData worksheet is not present.)

- **Optimization interval** is the time (simulation hours) between optimizations that derive the UAV allocations at that moment in time. (Optional: Defaults to 1.0)

- **Report interval** indicates the phases of the scenario for which measures of performance will be reported. Measures of performance for the overall scenario length are also provided in addition to these interval reports. (Optional: Defaults to 4.0)

2. Air Frame Worksheet

The AirFrame Worksheet contains all performance characteristics for each UAV. Each row in the worksheet represents one UAV. We varied the inputs at each row under the following columns: transition time, max speed (air speed), operating radius, operating time, and time horizon. The following list describes the column headings for the AirFrame worksheet (Ahner et al., 2006):

- **Type** is the class of UAV and may be used to ensure that a proper LRS is used for take off and landing.

- **Unit** is the owning military unit of the UAV listed on the same row and under the column Type.

- **Compatible GCS** indicates the type of GCS from the GCS Worksheet that is able to control this UAV. (Not used in the current version, but should not be deleted.)

- **Starting LRS** is the name from the LRSInput Worksheet of the LRS from which the UAV originates.

- **Ending LRS** is the name from the LRSInput Worksheet of the LRS to which the UAV lands. (Should be the same as the Starting LRS.)

- **Transition time** is the time, upon landing, that is required before the UAV is available to launch.

- **Max speed** is the travel rate of the UAV between locations.

- **Operating radius** is the max distance the UAV can be from a controlling GCS for effective control.

- **Name** is a unique name for the UAV.

- **StartAvail** is the time the UAV is initially available for launch, usually an H-hour.

- **EndAvail** is the time the UAV is last available in the scenario.

- **Operating time** is the maximum time the UAV may be away from an LRS.

- **Time horizon** is the time window used in the rolling algorithm of the optimization. Time horizon is usually 1 to 1.5 times the operating time plus transition time. This value is critical to determining what missions will be considered in the look-ahead time window to launch a UAV if GCS capacity is available.

E. ASC-U OUTPUT

ASC-U saves the simulation results as output reports in a Microsoft® Access® database. The output reports are organized into fourteen database tables. Table 7 provides a description for each report. For this thesis, we required the data contained in the Coverage and CoverageByType tables.

Table Name	Description
Coverage	The amount of time each mission is covered by a UAV
CoverageByType	The amount of time each mission is covered by each different type of UAV
CoverageDelay	The delay from the time a mission opens until it is first covered by a UAV
GCSLoadOverTime	The time average number of UAVs using each GCS in each time period
GCSUtilization	The time average load on each GCS
MissionAssignment	A schedule of which UAV is covering which missions
MissionPackageUtilization	The time average utilization rate of each type of MissionPackage at each LRS
RunInformation	Information about the DAFS version and data used to create the output tables
RVTCoverage	Not currently used
Schedule	A schedule of UAV sorties
TerseRVTCoverage	A summary of the coverage of each mission by each RVT
UAVReadyTimeOverTime	For each UAV, the amount of time it is ready for launch in each time period
UAVUtilization	UAV utilization data
UAVUtilizationOverTime	For each UAV, the proportion of ready time that the UAV was airborne in each time period

Table 7.   Measures of Performance Tables (From Ahner et al., 2006).

This chapter introduced the UAV allocation problem and the ASC-U simulation tool. We limited our discussion to the components of ASC-U that we used in our research. We also point out that ASC-U is in continuous development. During our research, the developers added several new functionalities involving sensor packages, UAV characteristics, and mission areas. We used ASC-U version 1.3.0 modified on April 13 10:41:11 PDT 2006 for our study.

THIS PAGE INTENTIONALLY LEFT BLANK

IV. ANALYSIS METHODOLOGY

This chapter discusses the analysis methodology employed in our research. We describe the selection of factors included in our experiment, the development of design points using Nearly Orthogonal Latin Hypercubes (NOLH), and the statistical software selected for the analysis.

A. MEASURE OF EFFECTIVENESS (MOE)

The ASC-U simulation supports the generation of a number of MOEs, including, percent mission coverage, percent mission type coverage, percent mission coverage by UAV type, UAV utilization, mission package utilization, coverage delay, percent AUTL (Army Universal Task List) coverage, Remote Viewing Station (RVT) coverage, and Ground Control Station (GCS) utilization. Other MOEs provide more detail that are summarized by these aggregate MOEs. An additional MOE supported by ASC-U is a term within the simulation-optimization process called *mission value*. Generated during the allocation of UAVs to mission areas, mission value is a quantifiable measurement that captures a UAVs service to a mission area. Since mission value is representative of the percent mission coverage and based on the mission payload, UAV type, and service time of a mission area, we felt that it would provide an appropriate measure into the overall performance of the simulation and quality of the schedule it produces.

B. DESIGN OF EXPERIMENT

The research conducted in this thesis takes advantage of experimental design techniques based on statistical theory and developed to assist researchers in the analysis of computer simulations (Kleijnen et al., 2005). The primary goal of experimental design is to assess how changes to input parameters (factors) affect the results (responses). We applied these techniques with runs of the ASC-U simulation tool in order to answer the research questions and provide insights into the model's development and application across a robust set of future mission scenarios.

The origins of Design of Experiments (DOE) have their roots in agricultural research in the early 1900s and have since captured the attention of several industries (Kleijnen, 2004). Original DOEs proved useful where only a few factors were considered in the investigation of the process in question. Recently, this "parallel experimentation" methodology has found its way into the pharmaceutical industry where process chemists are looking to enhance drug design and development (Henry, 2002). With the advent of faster computing power and increased appreciation for simulation applications, research analysts have begun to expand the application of DOE to simulations analysis (Kleijnen et al., 2005; Kelton, 2001).

1. Factor Selection

ASC-U relies on several types of input factors to model the scenario and process the allocation of UAVs to mission areas requiring different mission payloads. We selected factors that fell into two categories: UAV characteristics and performance capabilities, and optimization parameters.

The first set of factors we considered included the following UAV characteristics and performance capabilities: UAV type, sensor package, operating time, air speed, operating radius, and transition time. The UAVs considered at the time of the study included the Extend Range Multipurpose (ERMP) UAV, and the Future Force UAVs classified as Class I, II, III, and IV platforms. The base scenario used single values for operating time, air speed, operating radius, and transition times based on current and future projected UAV capabilities ("Unmanned Aircraft," 2005).

The second set of factors implemented within ASC-U involves the optimization. The factors include the optimization interval and the time horizon used to assess and assign UAVs to available mission areas. The optimization interval is set at a single value for the entire simulation run. The time horizon is used to identify the missions that become available for each type of UAV. This length of time can be viewed as a "planning window" that is specific to each type of UAV and is based on its operational capabilities. The simulation considers this future time horizon when allocating UAVs to mission areas at each optimization interval.

We based our final selection of the factors explored in the study on their relationship to the ASC-U solution and the research questions. The fact that ASC-U treats the assignment of UAVs as a dynamic routing problem indicated that influential factors would most likely consist of the platforms' characteristics and performance capabilities. This led to the selection of the following four factors for each type of UAV: operating time, air speed, operating radius, and transition time. Additionally, we selected the time horizon for each UAV based on its incorporation in the solution formulation and its potential impact on UAV assignments.

We selected the optimization interval as an additional factor. The optimization interval is a characteristic of ASC-U's optimization, rather than that of the platforms or the scenario. As the simulation proceeds, ASC-U queries the status of all UAVs and mission areas in order to optimize the allocation of UAVs to mission areas within their respective time horizons. The simulation tool uses the optimization interval to determine how often this query process occurs. An interval of 10, for example, conducts an optimization sequence every ten simulation hours. Our initial expectation was that the smaller the interval, the higher the overall mission value assigned to the scenario's schedule.

Our assessment of appropriate design factors led to the selection of 26 factors consisting of five factors for each UAV type and the simulation's optimization interval parameter. Table 8 displays the factors along with their base scenario values and the ranges used in the DOE. The ranges for the UAV factors were developed by adding and subtracting 20% of the base value. We set the range for the optimization interval between one and ten simulation hours.

UAV Types	Factors	Factor Name	Base Scenario Value	DOE Ranges	
				Low	High
ERMP					
	Time Horizon (hr)	EHoriz	36	28.8	43.2
	Operating Time (hr)	EOprT	36	28.8	43.2
	Air Speed (km/hr)	ESpeed	241	192.8	289.2
	Operating Radius (km)	ERadius	500	400	600
	Transition Time (hr)	ETrans	0.5	0.40	0.60
Class I					
	Time Horizon (hr)	1Horiz	0.83	0.664	0.996
	Operating Time (hr)	1OprT	0.83	0.664	0.996
	Air Speed (km/hr)	1Speed	93	74.4	111.6
	Operating Radius (km)	1Radius	8	6.40	9.60
	Transition Time (hr)	1Trans	0.16	0.128	0.192
Class II					
	Time Horizon (hr)	2Horiz	2	1.60	2.40
	Operating Time (hr)	2OprT	2	1.60	2.40
	Air Speed (km/hr)	2Speed	93	74.4	111.6
	Operating Radius (km)	2Radius	16	12.8	19.2
	Transition Time (hr)	2Trans	0.24	0.192	0.288
Class III					
	Time Horizon (hr)	3Horiz	6	4.80	7.20
	Operating Time (hr)	3OprT	6	4.80	7.20
	Air Speed (km/hr)	3Speed	222	177.6	266.4
	Operating Radius (km)	3Radius	40	32.0	48.0
	Transition Time (hr)	3Trans	1	0.80	1.20
Class IV					
	Time Horizon (hr)	4Horiz	6	4.80	7.20
	Operating Time (hr)	4OprT	6	4.80	7.20
	Air Speed (km/hr)	4Speed	231	184.8	277.2
	Operating Radius (km)	4Radius	75	60.0	90.0
	Transition Time (hr)	4Trans	0.5	0.40	0.60
ASC-U Parameter	**Factor**	**Factor Name**	**Base Scenario Value**	**Low**	**High**
	Optimization Interval	OptInt	1	1	10

Table 8.   Factors Based on UAV Performance Capabilities and their Ranges.

2.   Nearly Orthogonal Latin Hypercube (NOLH)

Once we selected the input factors, the next step was deciding how to assess the impact of the various levels for each factor against the MOEs generated by ASC-U. Without knowledge of experimental designs proposed by Kleijnen et al. (2005), an analyst may decide to start with only two or three factors set at the low and high levels. Using two levels for three factors would create eight design points. In order to gain a better understanding of the response surface, we would like to increase the number of factors and expand the levels for each.

Consider a full factorial experiment with our factors and three levels (low, middle, high) in order to identify non-linear relationships within the model. This would result in 3^{26} (2.54×10^{12}) design points. Since ASC-U is a deterministic simulation, only one run per design point would be required. Nevertheless, at approximately three hours per run, even with 1000 computers simultaneously executing a different design, it would take nearly nine-thousand centuries to acquire the data set. Fortunately, there are effective alternatives to using a full factorial design.

We selected the space-filling design of Nearly Orthogonal Latin Hypercubes (NOLH) to provide an exploration of the outer and interior regions of the response surface. NOLH designs allow the analyst to develop a comprehensive set of explanatory variables represented in the model (Cioppa, 2002). Instead of being restricted to two or three levels, the analyst can create a design that uses multiple levels or even a continuous range of values for each factor. This facilitates the identification of non-linearities within the response surface (Brown, 2000).

In addition to good space-filling properties, orthogonality is another desirable property of designs. Orthogonal designs have no linear relationship between the regressors (Montgomery, Peck, & Vining, 2001). The NOLH technique minimizes the correlation between factor columns, creating a nearly orthogonal design matrix. We can examine the off-diagonal elements within the correlation matrix of the design in order to measure the level of orthogonality. The spreadsheet design tool described below has several features that guard against multicollinearity and produce a robust space-filling design.

Using the NOLHdesigns_v4.xls spreadsheet developed by Professor Susan M. Sanchez, we generated 257 design points consisting of 26 factors (Sanchez, 2005). The spreadsheet in Figure 14 consists of worksheets that create designs for a specific number of factors. Since our experiment called for 26 factors, we used the worksheet that creates a nearly orthogonal design for 22-29 factors. The spreadsheet employs the algorithm described by Cioppa (2002) where the maximum number of factors examined in a Latin hypercube is $m + \binom{m-1}{2}$ and m is an integer greater than 1. Solving for m using 29 as the number of factors gives $m = 8$. The number of n design points required is given by $n = 2^m + 1$ and results in 257 (Cioppa, 2002).

Figure 14.   Nearly Orthogonal Latin Hypercube (NOLH) Design Spreadsheet.

Our final design consisted of a 257 x 26 matrix with the largest correlation of 0.0816. Figure 15 provides the two-dimensional projections for the optimization interval and ERMP factors, which display the space-filling properties of the design. We created Microsoft® Visual Basic® macros to generate 257 scenario templates in Excel® and transfer the respective design points to each one. At this point, we were ready to begin our runs.
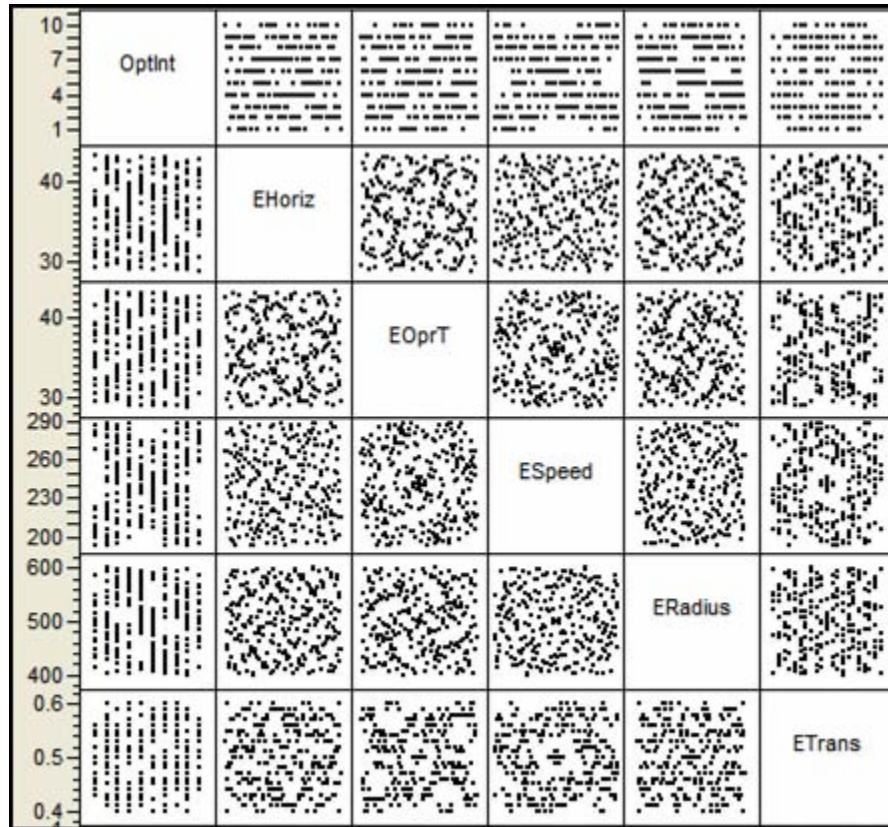
Figure 15.   Scatterplot Matrix for Optimization Interval and ERMP Factors.

3.   Computing Resources

Simulation analysis requires scenario productions runs. Simulations involving stochastic processes require multiple runs per scenario. For example, a simulation with 257 design points may require 50 runs each. This amounts to 12,850 runs for a single data set. Researchers often look to supercomputing clusters to support their simulation

requirements. Two organizations that facilitate data farming in this way are the Maui High-Performance Computing Center (MHPCC) at the University of Hawaii and the MITRE Corporation in Woodbridge, VA (Wolf, 2003; Hakola, 2004). A script is usually created to transfer each row of the design point to a single simulation run. Our computer resource needs were different in two ways.

First, ASC-U is a deterministic simulation requiring only one run per design point. This limited the number of runs that we needed to 257. Second, ASC-U uses a graphic user interface (GUI) to load each design point and initiate a run. Once the simulation is complete, the analyst saves the results to a Microsoft® Access® database. While we would have liked to create a script to automate the run-initiation process, we found that, based on time constraints, it was easier to initiate each run manually for our study. At approximately three hours per run, we require over 700 hours of processing time. We used the computer labs in the Operations Research Department, Naval Postgraduate School, Monterey, CA to complete our simulation runs. We employed approximately 60 computers simultaneously to load and initiate each run. The computing resources consisted of Dell 2.80 GHz Pentium 4 Computers with 1.00 GB RAM running Microsoft® Windows® XP Professional.

C.   ANALYSIS OF THE DATA

This section describes the data consolidation process and statistical software package used in the study. We were interested in ways to facilitate our current as well as future studies involving the ASC-U simulation tool. Efforts were made to develop a DOE methodology that could be integrated with ASC-U. Additionally, we desired a user-friendly data analysis package that facilitated analysis and provided a graphical display of intermediate and final results.

1.   Data Consolidation

ASC-U provides the ability to write the results in several different database structures. Since the results from trial runs were too large for Excel® to handle, we saved the outputs to Microsoft® Access® databases. We generated 257 databases after

completing the runs. Each database was approximately 30 megabytes in size, with 14 tables comprised of MOE data and a UAV flight schedule. Our task was to extract the desired MOEs and consolidate the results with the original design matrix.

We determined that it was beneficial to extract the percent mission type coverage, percent mission coverage by UAV type, and the mission value generated for each run. The data required to calculate these MOEs reside in two tables: Coverage and CoverageByType. Since the Coverage table consisted of 21,360 rows, we converted the table to Excel® format. We created Visual Basic® macros to calculate the percent mission type coverage for all mission payloads and the mission value for each design point. Using the same set of macros, we extracted the MOEs and consolidated them with the original design spreadsheet.

The CoverageByType consists of 106,800 rows and is therefore too large to save as an Excel® file. A short application was created in Java™ using the Java Database Connectivity (JDBC) to access the CoverageByType table within Microsoft® Access®, calculate the percent mission coverage by UAV type, and output the results as a comma separated value (.csv) file. The Java™ code is displayed in Appendix E. The results were merged with the design matrix, creating a row for each design point with 20 additional columns for the MOEs.

2. JMP Statistical Discovery Software™

In order to facilitate our analysis, we selected JMP Statistical Discovery Software™ from SAS. JMP Software provides a stand-alone analytical tool for DOE development, implementation, visualization and analysis. The research analyst can learn the fundamentals within JMP in order to input, manipulate, and begin analysis of their data within a few hours. JMP provides the following capabilities that were specifically useful during our research:

- Spreadsheet environment for entering, editing, and displaying data sets.
- Interactive graphs and reports that assist in the exploration of the data.
- Journaling tools that record the investigative process for follow-on review.

In closing, a space-filling design coupled with a robust software package assisted our exploration of the response surface represented by the multiple Measures of Effectiveness (MOE) depicted in the solution of ASC-U.

V.   DATA ANALYSIS

This chapter describes the analysis of our data. Section A provides an overview of the techniques used during the analysis. In Section B, we provide an assessment of our first design and the data characteristics that led to the development of a new design. We continue with initial observations of the data generated by the new design using histograms and a scatter plot of the mission value by design points.   Section C provides an in-depth analysis of the regression model using mission value as the response variable. Section D develops an alternate regression model using percent mission coverage as the response variable. In Section E, we describe interesting observations by comparing the measures of effectiveness used in our two models and provide an interpretation of our model coefficients.

A.   MULTIPLE REGRESSION ANALYSIS

Multiple regression analysis creates a mathematical description of the relationship between a dependent variable (y) and several independent variables (x) (Devore, 2004). We call the dependent variable the response and the independent variables regressors. The technique involves predicting (fitting) the response variable using a linear combination of the regressors. The linear model is described in two forms, the true model and the estimated model. The true model is a representation of the actual observed values. The estimated model represents the predicted or expected values. We enumerate the regressors as x_1, x_2, …, x_k, where k represents the number of regressors ($k >= 2$). The model also includes parameters β and ε. The parameters β_1, β_1, …, β_k are coefficients that represent the amount the response variable changes when the corresponding regressor changes by one unit. The intercept, β_0, is a constant where the regression line intercepts the y-axis. Error in the true model is represented by ε. It is the difference between the actual value and its predicted value. In the estimated model, the difference is called a residual (Sall, Creighton, & Lehman, 2005). Figure 16 displays the components of a general linear model with two terms.
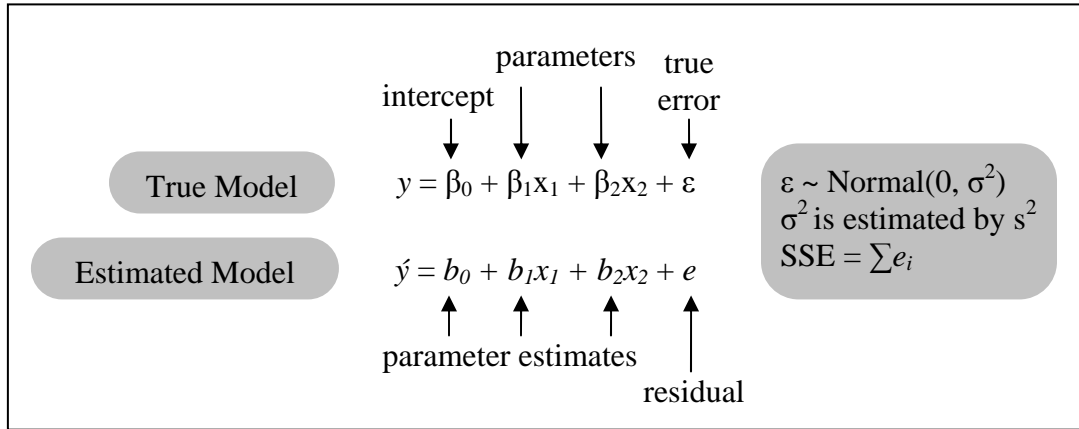
Figure 16.   Components of a General Linear Model (After Sall et al., 2005).

Figure 16 represents a first-order model. However, variations of the regression model may also include second-order terms (polynomial) to investigate curvilinear effects, cross-product terms (factorial) to investigate interaction effects, and full quadratic models that combine both second-order and factorial terms in one equation. Creating full quadratic models during regression analysis may result in a robust model that is able to explain a larger portion of the variation in the response variable compared to a simple first-order model. Figure 17 displays four multiple regression models using two independent variables.

Figure 17.   Multiple Regression Models.

To conduct meaningful regression analysis, we must verify certain assumptions about the data set. First, there must be at least an approximate linear relationship between the response variable and the regressors. Analysts check this relationship by overlaying a graph of the regression equation on the scatter plot of the data (Devore, 2004). Next, the residuals must have a zero mean and constant variance. Finally, the residuals must be normally distributed. Analysts can use histograms and Normal quantile plots to check the Normality assumption. JMP uses the *Shapiro-Wilk test* (*W-statistic*) to test Normality when n <= 2000 (Sall et al., 2005).

The JMP statistical software package reports the *t*-ratio and corresponding *P*-value for each regressor in the model. JMP uses the *t*-ratio to test the contribution of each regressor. The procedure tests the significance of an individual regression coefficient, β_j. The null hypothesis H_0: $\beta_j = 0$ is rejected over the alternate hypothesis H_1: $\beta_j \neq 0$ if $|t_o| > t_{\alpha/2, n-k-1}$. If the alternate hypothesis is accepted, then we conclude that the regressor x_j is significant given the other regressors remain in the model. (Montgomery et al., 2001) The *t*-statistic is calculated using the standard error for the slope, se($\hat{\beta}_i$):

$$t_o = \frac{\hat{\beta}_i}{se(\hat{\beta}_i)}$$

Multiple regression analysis allows the analyst to identify a set of regressors that explain a proportion of the variance in the response variable. The level at which the regressors explain the variance of the model is established with a significance test of R-square (R^2). R-square is calculated using the sum of squared residuals (SSE) and the total sum of squares (SST):

$$R^2 = 1 - \frac{SSE}{SST}$$

The analyst can use an Adjusted R-square (R_a^2) to compare models with different numbers of parameters (*k*). The Adjusted R-square is calculated using the mean squared error [MSE = SSE/(n-(k+1))] and the mean square of treatments [MST = SST/(n-1)]:

$$R_a^2 = 1 - \frac{MSE}{MST}$$

Another method used to compare regression models is called the *F* test. The analyst builds two models consisting of different numbers of regressor variables. The full model contains more regressors (*k*) than the reduced model with *l* regressors. Since the full model consists of additional regressors, it should fit the data as well or better than the reduced model. The *F* test uses the sum of squared residuals for the full model (SSE_k) and the reduced model (SSE_l) to calculate the value of the *f*-statistic. The full model is rejected over the reduced model if $f \geq F_{\alpha, k-l, n-(k+1)}$ (Devore, 2004).

$$f = \frac{(SSE_l - SSE_k)/(k-l)}{SSE_k / [n - (k+1)]}$$

We used stepwise regression to assist in model development due to the number of regressors in our study. JMP allows the analyst to select between backward elimination, forward selection and mixed stepwise regression. We selected mixed stepwise regression for our analysis. The procedure begins with forward selection by adding variables one at a time based on the one that generates the largest absolute *t*-ratio when it enters the model. After adding a regressor to the model, it examines the previously entered variables for the smallest absolute *t*-ratio. JMP compares the corresponding *P*-value for the candidate *t*-ratios to user-defined probabilities to enter or leave the model, and processes them respectively. The process stops when variables are no longer significant (Sall et al., 2005).

B.   INITIAL OBSERVATIONS

Our first design consisted of 26 factors resulting in a 257 x 26 design matrix. In this design, the optimization interval contained ten levels from one to ten simulation hours. Prior to running our design, we predicted that the optimization interval would have a large impact on the overall mission value and mission percent coverage. We believed that the smaller the interval, the larger the mission value generated with all other factors remaining constant. We based our prediction on the assignment process within ASC-U. The more frequently ASC-U initiates an optimization sequence, the less it misses "windows of opportunity" for missions that become available. Thus, the simulation is able to reallocate UAVs to gain a higher mission value and increase the percent mission coverage. However, because shorter optimization intervals require longer ASC-U run times, we were interested in finding out how rapidly the solution degraded when the optimization interval increased.

We started our analysis by fitting the main effects using the stepwise regression feature in JMP. The direction of the regression was set to "mixed" with "combined" rules so that the regressors that entered into the model on previous steps are reassessed in subsequent steps. We set the probability to enter and leave at 0.050 and 0.100, respectively. Figure 18 displays the actual value by predicted plot and summary statistics of the results.
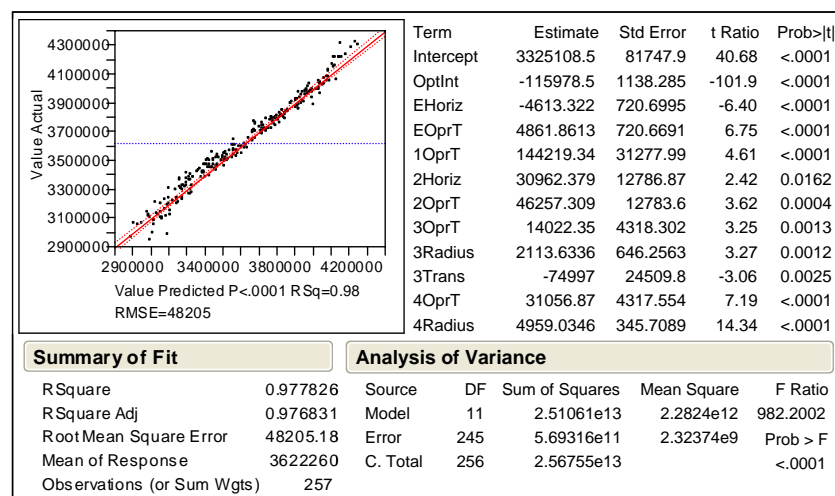
Figure 18.   Actual Value by Predicted Plot and Statistics for Initial DOE.

The stepwise process selected eleven factors: OptInt, EHoriz, EOprT, 1OprT, 2Horiz, 2OprT, 3OprT, 3Radius, 3Trans, 4OprT, and 4Radius. We continued with a standard least squares regression on the eleven main effects.

To our surprise, a simple regression of 11 main effects explained 98% of the variance within the model. We were eager to investigate the significance of the factors using the visual screening tool provided by JMP called the Prediction Profiler. The Prediction Profiler allows the analyst to explore the effect on the predicted response variable by changing one or more factor settings (Sall et al., 2005). The importance of the optimization interval was evident upon viewing the plots displayed in Figure 19.
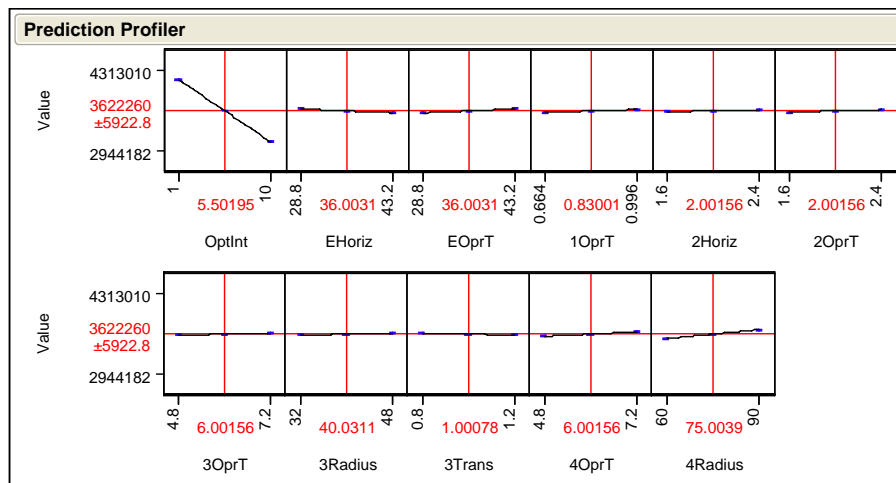
Figure 19.   Prediction Profiler for Initial DOE.

In Figure 19, we see that the optimization interval dominates the other factors with its effect on the response. While this initial finding confirmed our earlier prediction, we quickly realized that the optimization interval's strong effect was going to limit our ability to assess the other factors' influence on the model. Prior to considering alternate options for our analysis, we ran a simple regression using the optimization interval as the only regressor in order to find out how much of the model it explained. Figure 20 displays the results of the one-term model. The regressor accounted for 94% of the variance within the model.

Actual by Predicted Plot
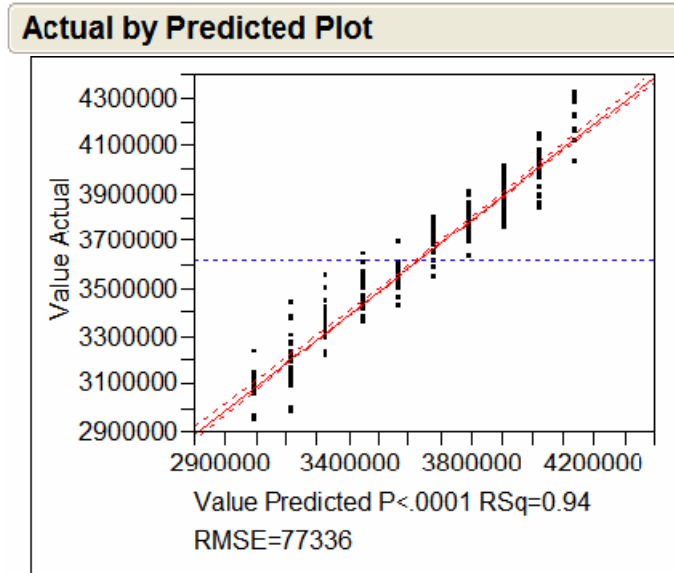
Figure 20.   Actual by Predicted Mission Value Plot for Initial DOE.

Not only does optimization interval explain "almost all" of the variation, but the mission values for larger optimization intervals show a reduction in the overall mission value by nearly 50%. This is clearly unacceptable. The practical implication is that for this scenario, ASC-U should be used with a short optimization interval in order to obtain a good solution, even though this requires more computing time.

The dominant influence of the optimization interval led us to explore other options for our analysis. Our goal was to eliminate the presence of the interval's effect and examine the other twenty-five factors. We looked at our design of experiment to see how many runs consisted of the optimization interval set to one. There were fifteen instances, not enough for the number of predictor variables in our study. Tabachnick and Fidell (1989) propose the rule of thumb for testing R-square using $N >= 50 + 8m$, where N = number of observations and m = number of predictors. Since we were interested in the effects of the twenty-five UAV factors, we needed a sample size nearly the size of our original design. Otherwise, a situation where $m >= N$ results in a trivial solution of R-square $= 1.0$.

We generated a new design of experiment using the twenty-five UAV factors. We concatenated the 15 runs from the original design with the 257 new runs. The result was a maximum pairwise correlation of 0.0372, providing nearly orthogonal properties for our design (Cioppa, 2002). We generated the new data set and combined the results with the original fifteen runs, giving us 272 observations for our analysis.

Once we completed the runs for the new design, we computed the mission values and twenty MOEs. We consolidated the results with their corresponding design points using the methodology described in Chapter IV. Our initial assessment consisted of reviewing the distributions of the MOEs as displayed in Figures 21-23. Figure 21 displays the distribution and summary statistics of the mission value for all 272 designs. The base scenario design generated a mission value of 4224154, slightly above the mean of 4215522. Many of the MOEs are approximated by a normal distribution, with the base scenario falling in the center of the data. However, several MOEs present a bimodal distribution that warrant further investigation.
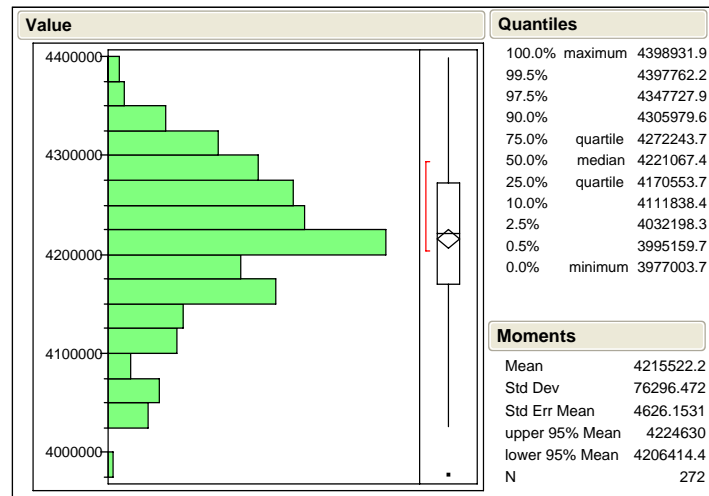
Figure 21.   Distribution and Summary Statistics of Mission Value.
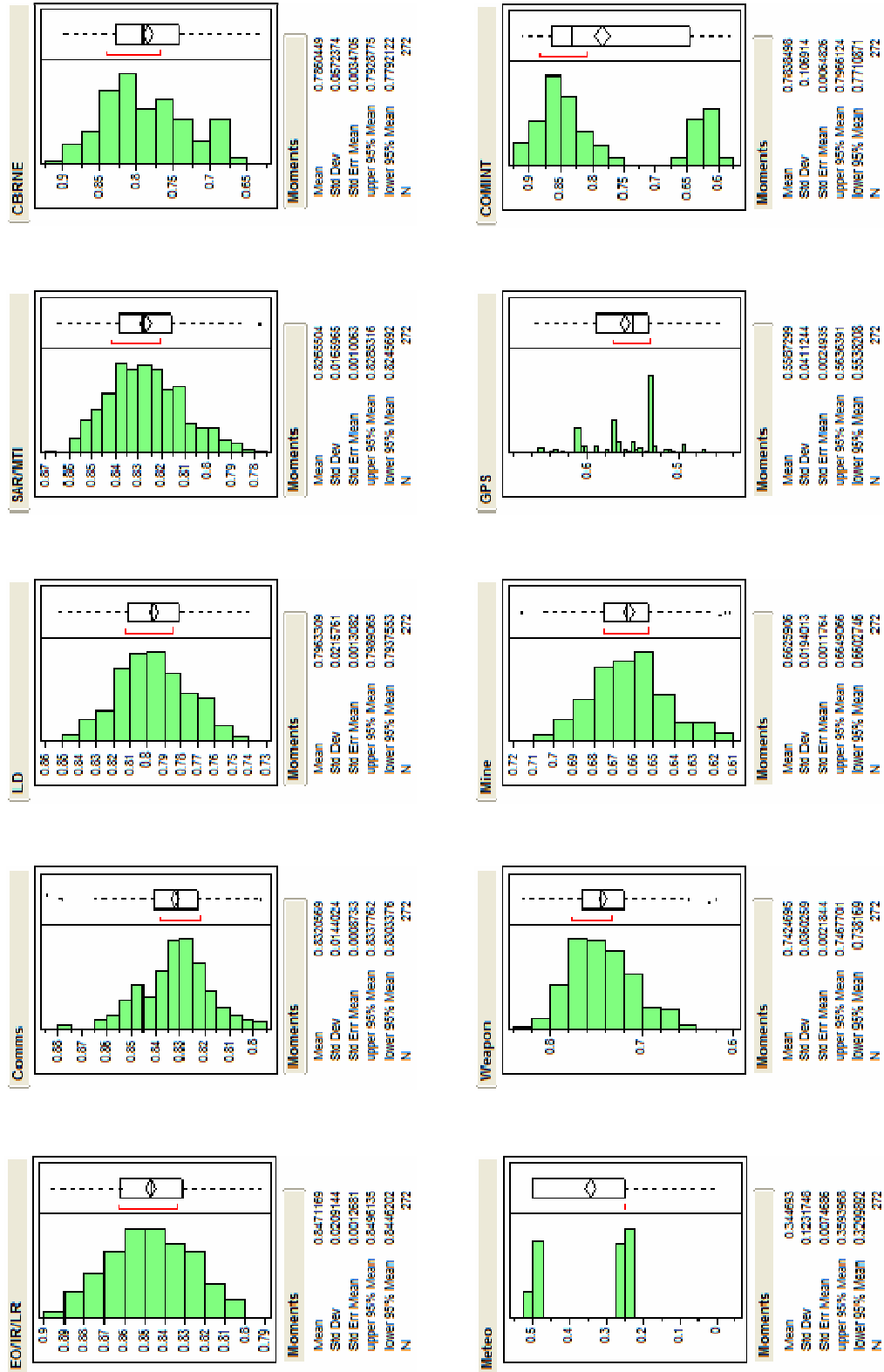
Figure 22. Distribution and Summary Statistics for MOEs.
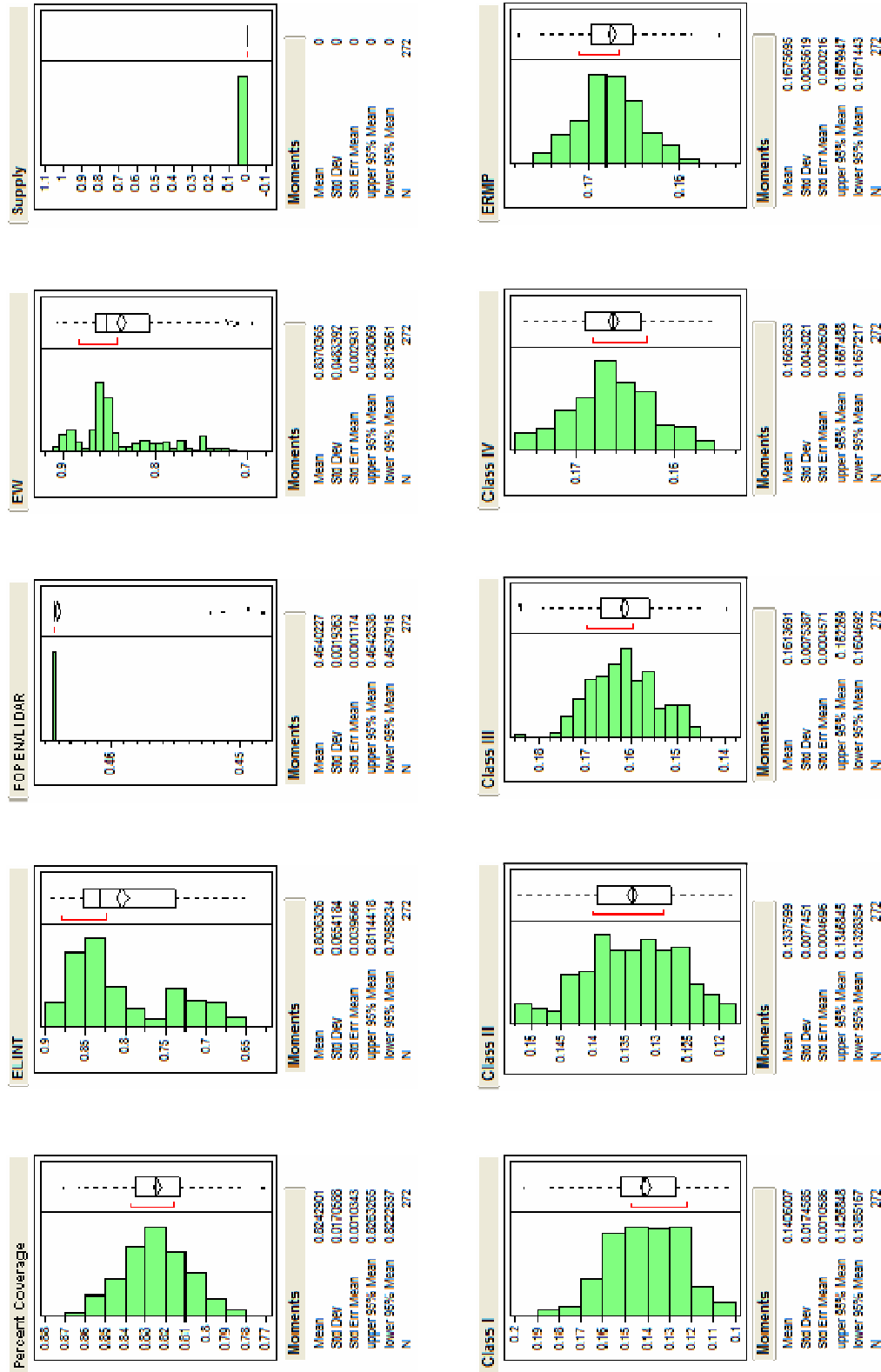
Figure 23.   Distribution and Summary Statistics for MOEs.

Of particular interest are the percent coverage distributions for the following payloads: meteorological (Meteo), communication intelligence (COMINT), foliage penetrating radar/light detection and ranging (FOPEN/LIDAR), and supply delivery (Supply). We investigated the significant individual factors that influence the behavior of the first two MOEs forming bimodal distributions. We identify the factor(s) that tend to cause the MOEs to concentrate into separate regions. Our preliminary findings for Meteo and COMINT are displayed in Appendices C and D, respectively. The last two MOEs have little to no variation in their percent coverage. FOPEN/LIDAR predominantly receives a percent coverage of 46.4%, whereas the solution does not allocate UAVs to supply delivery missions. We investigate FOPEN/LIDAR coverage and supply delivery missions in Section E of this chapter.

After reviewing the histograms for each MOE, we generated the scatterplot for mission value in Figure 24. We observed one design point, 140, falling below 3.13 standard deviations from the mean. Additionally, we were particularly interested in the five extreme values located at the top of the plot achieving high overall mission values. In the next section, we discuss the regression analysis that investigates these observations further.
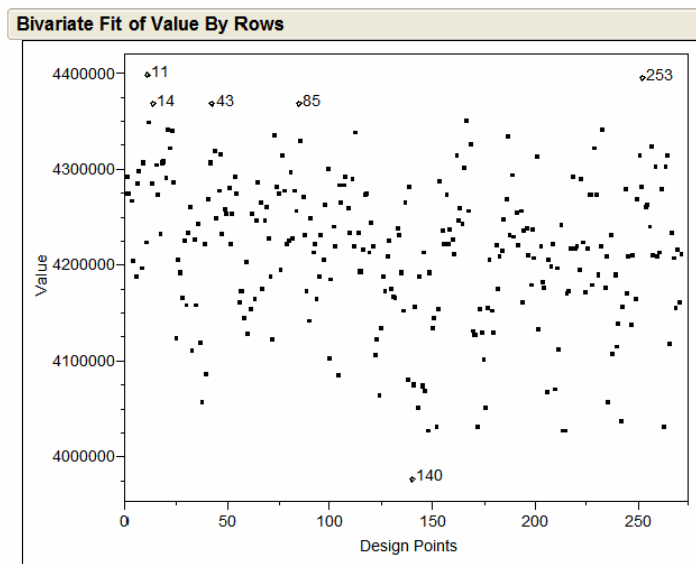
Figure 24.   Scatterplot of Mission Value for Design Points.

C. MISSION VALUE MODEL

This section provides an analysis of the regression model using mission value as the response variable. We were interested in the effects that the UAV characteristics and performance capabilities had on the ASC-U generated mission value for each scenario.

1. Main Effects Model

We started our analysis with a mixed stepwise regression on the main effects using a probability to enter and leave of 0.050 and 0.100 respectively. The stepwise process selected 12 of the 25 regressors: EHoriz, EOprT, 1Horiz, 2OprT, 1Radius, 2Radius, 3Horiz, 3OprT, 3Radius, 4Horiz, 4OprT, and 4Radius. We performed a standard least squares regression on the selection. Figure 25 displays the actual value by predicted plot for the regression. The model generated an R-square value of 0.8895. Eight of the twelve factors were significant with a Prob>|t| <0.0001. Three more were significant at 0.0061 or less. One factor, 2Radius, generated a Prob>|t| of 0.0265.
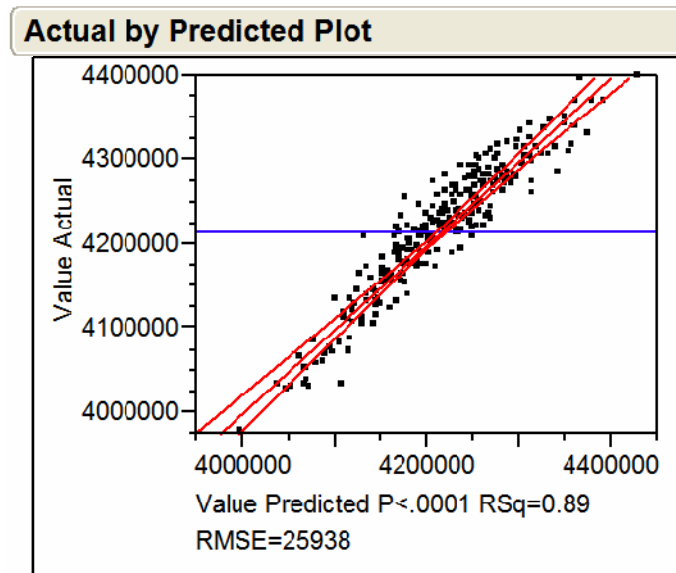
Figure 25.   Actual by Predicted Mission Value Plot for Main Effects Model.

2. First Order Model with Interactions

We would like to increase the explanation of the variance within the model and at the same time keep the significant factors to a minimum. In order to establish a range of R-square values, identify significant factors, and further investigate trends within the data, we generated a first order model with interactions. We started with all main effects. Next, we ran the macro within JMP to add effects with factorial to degree set at 2. We performed a stepwise regression followed by least squares regression as described above.

Figure 26 displays the actual value by predicted plot for the regression. Again, we notice a high level of stability between the predicted plot and the actual data. The stepwise process selected 20 main effects and 24 interaction terms. The model generated an R-square value of 0.9557. Nineteen of the factors were significant with a Prob>|t| <0.0001. Ten of the factors generated a Prob>|t| greater than 0.0100. Interestingly, each UAV type presented four of five factors within the model. Air speed was not selected for ERMP, Class II, and Class III UAVs. Transition time was not selected for Class I and Class II UAVs. We will investigate the selection of significant factors as we reduce the number of regressors to develop the final model.
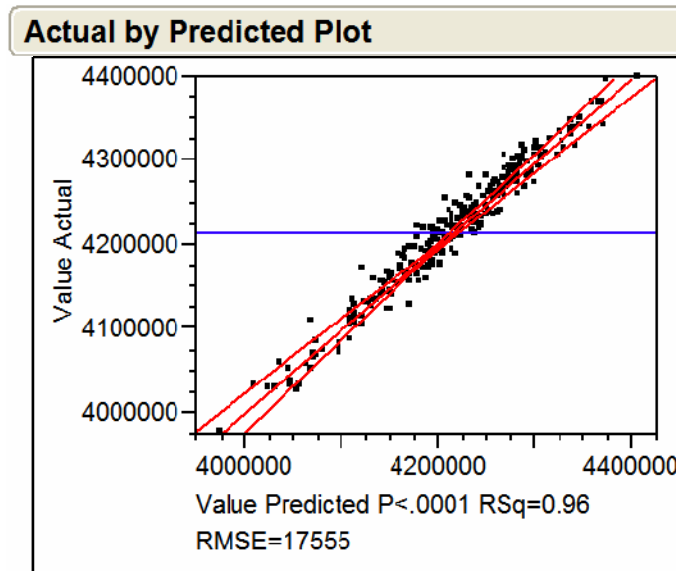
Figure 26.   Actual by Predicted Mission Value Plot for First Order with Interactions.

63

3. Full Quadratic Model

At this stage, we combined our model forms to create a full quadratic model with main effect, polynomial, and interaction terms. We employed the same techniques as described above by using JMP to add main effects and interaction terms. JMP also provides a macro to add polynomial terms to a user-defined degree setting. We selected polynomial to degree set at 2. Prior to selecting stepwise regression on our model effects, we changed the probability to leave from 0.0100 to 0.0500. This was done in order to eliminate excessive terms that had a Prob>|t| greater than 0.0100. Our first order interaction model had ten such effects that did not significantly explain the model.

Figure 27 displays the actual value by predicted plot for the full quadratic model. The stepwise process selected 35 significant factors consisting of 19 main, 11 interaction, and 5 second-order terms. The model generated an R-square value of 0.9610. Sixteen of the factors were significant with a Prob>|t| <0.0001. Fourteen of the factors were significant at 0.0080 or less. Five of the factors generated a Prob>|t| greater than 0.0100, half the amount found in the first order interaction model.
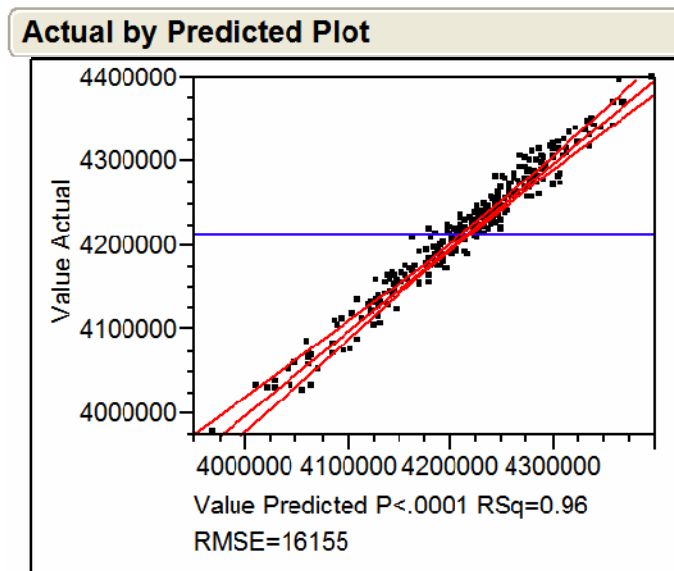
Figure 27.　　Actual by Predicted Mission Value Plot for Full Quadratic Model.

4. Final Model

We evaluated the step history generated in the stepwise regression of the full quadratic model in order to construct the final model consisting of nine main effects, one interaction term, and one second-order polynomial term. The statistical report for the regression model for mission value is displayed in Appendix A. JMP provides the R-square values produced by the remaining terms in the model at each iteration of the stepwise process. Table 9 displays the significant model terms and corresponding R-square values. Next, we evaluated the R-square values at the "knee in the curve" displayed in Figure 28 using the F test described previously in this chapter.

Terms	Parameter	R-Square
1	4Radius	0.52544
2	1OprT	0.67606
3	EHoriz	0.76483
4	EOprT	0.81134
5	(EHoriz-35.9408)*(EOprT-35.9651)	0.82657
6	3Radius	0.84766
7	1Radius	0.86559
8	(4Radius-75.0007)*(4Radius-75.0007)	0.89281
9	4Horiz	0.90568
10	3Horiz	0.91541
11	4OprT	0.92098
12	1Horiz	0.92458
13	3OprT	0.92889
14	(3Horiz-6.00654)*(3OprT-5.98118)	0.93172
15	(EOprT-35.9651)*(EOprT-35.9651)	0.93652
16	1Speed	0.93808
17	2Radius	0.94023
18	2OprT	0.94130
19	(2OprT-1.99919)*(4OprT-6.00765)	0.94293
20	(EHoriz-35.9408)*(4Radius-75.0007)	0.94445

Table 9.   Significant Model Terms and Corresponding R-square Values for Mission Value Model.
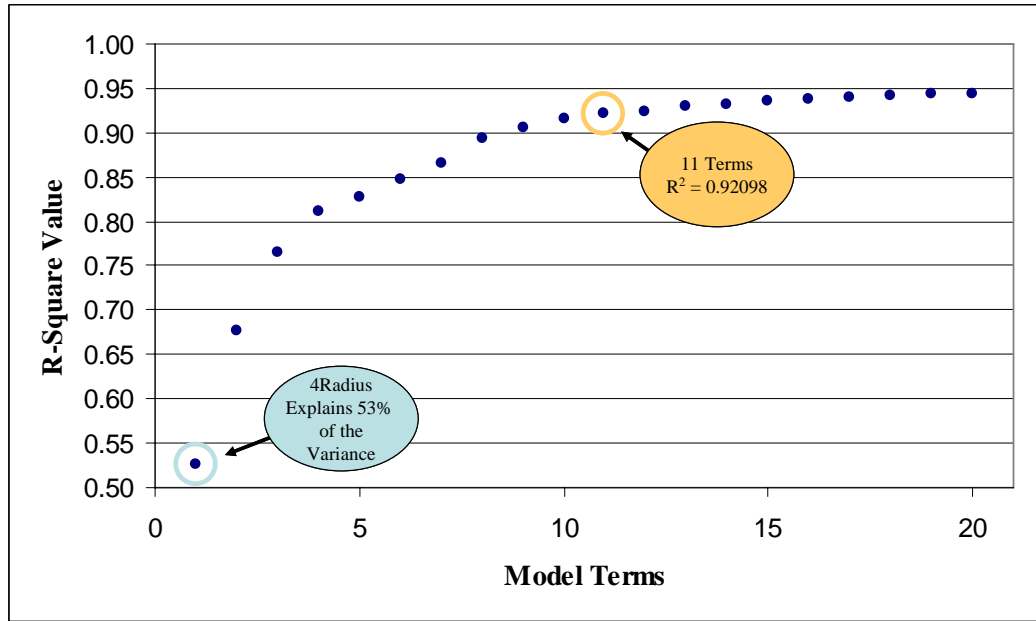
Figure 28.   R-Square Value and Corresponding Terms from Stepwise History for
Mission Value Model.

Our goal was to maintain a meaningful explanation of the variance within the model and keep the significant factors to a minimum. While R^2 provides a measure of the explained variance within a given model, it can be misleading when the model contains many regressors compared to the size of the sample (Devore, 2004). We explored the addition of each term to the model using the model utility F test. With the F test, we can develop an assessment as to whether additional predictors provide a significant increase to the explanation of the model (Devore, 2004).

Table 10 displays the sequential F test for the full model containing all twenty remaining terms from the stepwise history. The right-hand side of the table displays the critical values for the F Distribution for a test with α set at 0.0001, 0.0010, 0.0100, and 0.0500 for comparison. For the study, we were interested in the level of significance with α = 0.0001. As we move down the table, we are adding predictors and interested in the case where the f-statistic is less than the F critical value for the first time. For our model, this occurs when adding the twelfth regressor. We conclude that the addition of the first eleven regressors contribute significantly to the model.

66

n =	272	numerator	denominator		$F_{a,k-l,n-(k+1)}$			
Terms	SSE	df	df	f	0.0001	0.0010	0.0100	0.0500
1	7.49E+11							
2	5.11E+11	1	269	125.07435	15.6003	11.0693	6.7300	3.8763
3	3.71E+11	1	268	101.16488	15.6021	11.0702	6.7304	3.8764
4	2.98E+11	1	267	65.80961	15.6039	11.0712	6.7307	3.8765
5	2.74E+11	1	266	23.36293	15.6057	11.0721	6.7311	3.8767
6	2.40E+11	1	265	36.69850	15.6075	11.0730	6.7315	3.8768
7	2.12E+11	1	264	35.20091	15.6093	11.0740	6.7318	3.8769
8	1.69E+11	1	263	66.79908	15.6111	11.0749	6.7322	3.8771
9	1.49E+11	1	262	35.74072	15.6130	11.0759	6.7326	3.8772
10	1.33E+11	1	261	30.03970	15.6149	11.0769	6.7330	3.8773
11	1.25E+11	1	260	18.30804	15.6167	11.0778	6.7334	3.8775
12	1.19E+11	1	259	12.35303	15.6186	11.0788	6.7337	3.8776
13	1.12E+11	1	258	15.66285	15.6205	11.0798	6.7341	3.8778
14	1.08E+11	1	257	10.63874	15.6225	11.0808	6.7345	3.8779
15	1.00E+11	1	256	19.35920	15.6244	11.0818	6.7349	3.8780
16	9.77E+10	1	255	6.43972	15.6264	11.0828	6.7353	3.8782
17	9.43E+10	1	254	9.12737	15.6283	11.0838	6.7357	3.8783
18	9.26E+10	1	253	4.61943	15.6303	11.0849	6.7361	3.8785
19	9.00E+10	1	252	7.18978	15.6323	11.0859	6.7365	3.8786
20	8.76E+10	1	251	6.87798	15.6343	11.0870	6.7369	3.8788

Table 10.   Model Utility *F*-test for Twenty Terms Selected in the Stepwise Regression for the Mission Value Model.

Figure 29 displays the actual value by predicted plot for the final model consisting of 9 main effects, 1 two-way interaction, and 1 second-order polynomial. The eleven terms account for 92% of the variance within the model. Two predictors accounted for nearly 68% of the variance within the model: Class IV operating radius at 53%, and Class I operating time for another 15%. All of the factors were significant with a Prob>|t| <0.0001. Before exploring the significant factors and interactions, we verified the model's validity.

Recall that the model's summary statistics such as the *t* and *F* ratios as well as the R^2 value depend on several assumptions. We checked the validity of the assumptions by first investigating the actual value by predicted plot. Figure 29 indicates that the relationship between the response variable and the regressors is linear. Next, we confirmed that the residuals displayed a mean of zero and constant variance by observing the residual by predicted value plot in Figure 30. Finally, we checked the normality assumption with a histogram and Normal quantile plot of the residuals displayed in Figure 31. The plots, along with a *Shapiro-Wilk* value of 0.99 at a significance of 0.46, indicate that we can safely assume the residuals meet the Normality assumption.
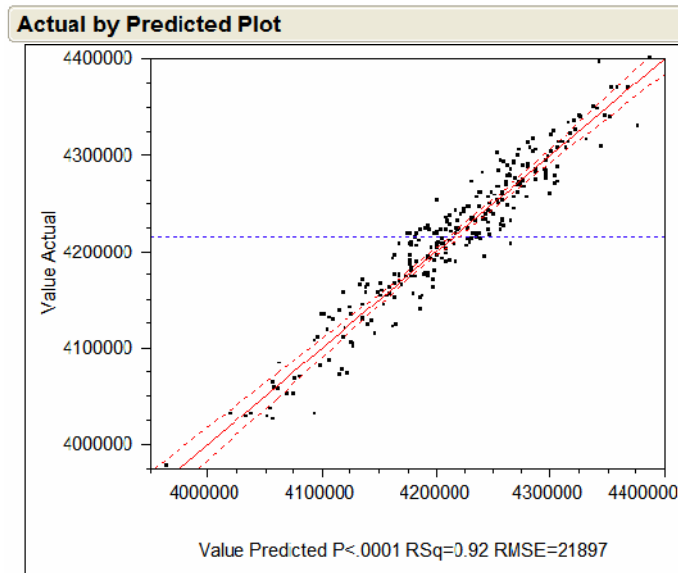
Figure 29. Actual by Predicted Value Plot for Final Mission Value Model.
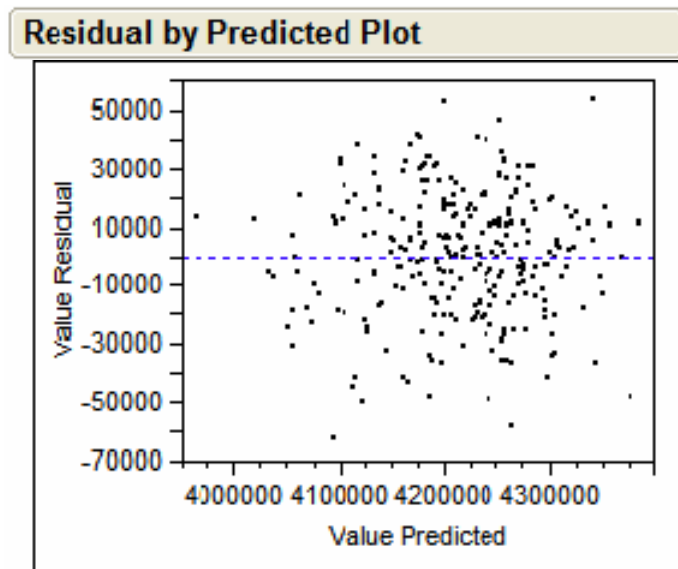
Figure 30. Residual by Predicted Value Plot for Final Mission Value Model.
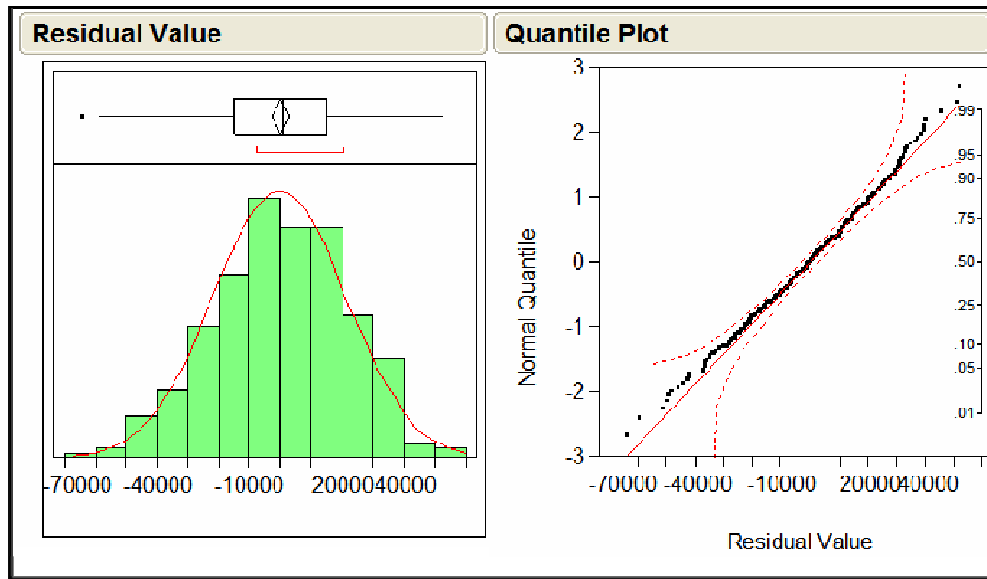
Figure 31.   Histogram and Normal Quantile Plot of Residuals for Final Mission Value
Model.

5.   Significant Factors

As mentioned in the previous section, Class IV operating radius and Class I operating time explained 68% of the variation in the mission value. In Section B, we saw that the optimization interval dominated the other factors with its effect on the response. Our new design, with the optimization interval set at one, presents significant findings involving other factors. The Prediction Profiler in Figure 32 indicates that Class IV operating radius has the strongest effect on mission value. Class I operating time, ERMP time horizon and operating time provide a lesser effect. The remaining main effects demonstrate a weak effect on the response.

The second-order polynomial term for Class IV operating radius also introduces a curvilinear effect. While an increase in the Class IV operating radius tends to increase the overall mission value, there is a point of diminishing returns. We also note that there is a direct relationship between Class IV operating radius and mission value. The same trend occurs for Class I operating time and mission value. However, ERMP time horizon demonstrates an inverse relationship with mission value. We explore this counterintuitive effect later in this section.
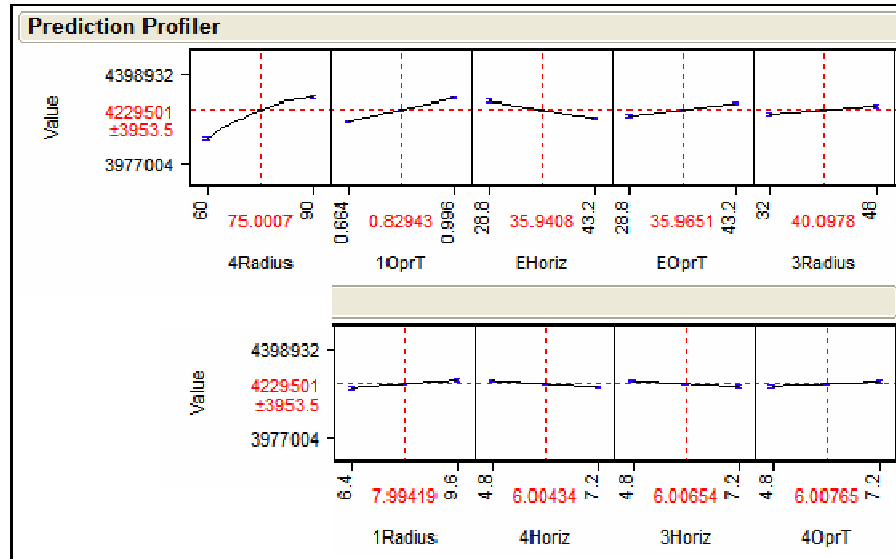
Figure 32.   Prediction Profiler for Final Mission Value Model.

We explored the significant factors further using JMP's partitioning platform. JMP allows the analyst to generate regression trees as a method of exploratory modeling. Regression trees employ a binning and averaging process. The software's algorithm evaluates all of the predictor values in order to determine the optimum split in the tree. The predictor value that generates the highest reduction in total sum of squares is selected to create the branch in the tree (Sall et al., 2004).

Figure 33 displays the regression tree for mission value after the first two splits. In the first split, the tree indicates that when Class IV aircraft have an operating radius of greater than or equal to 68.9 km, the overall mission value tends to be higher. In fact, the mean of the resulting mission value represents an increase by 8.2% of the total mission value range generated by our design. This also corresponds to a two percent increase over the mission value of the baseline scenario. The Class I operating time variable generates the second split. For UAV configurations where Class IV aircraft have an operating radius above 68.9 km, Class I operating time is the best predictor of mission value. Class I platforms with an operating time greater than 0.901 hrs increase the mean mission value by 18.5% of the total mission value range. The significance of this finding is that by considering levels for only two airframe factors out of twenty-five, we can

70

increase the mean of the mission value by nearly 19%. Additionally, an increase in the Class I UAV's operating time by at least 4.26 minutes (8.5% of the base scenario setting) accounted for more than a ten percent increase to the mean mission value. Perhaps even more interesting, it appears that improvements to the mean mission value can be achieved even if the Class IV UAV operates with a maximum radius that is 6.1 km smaller than established by the base scenario setting.
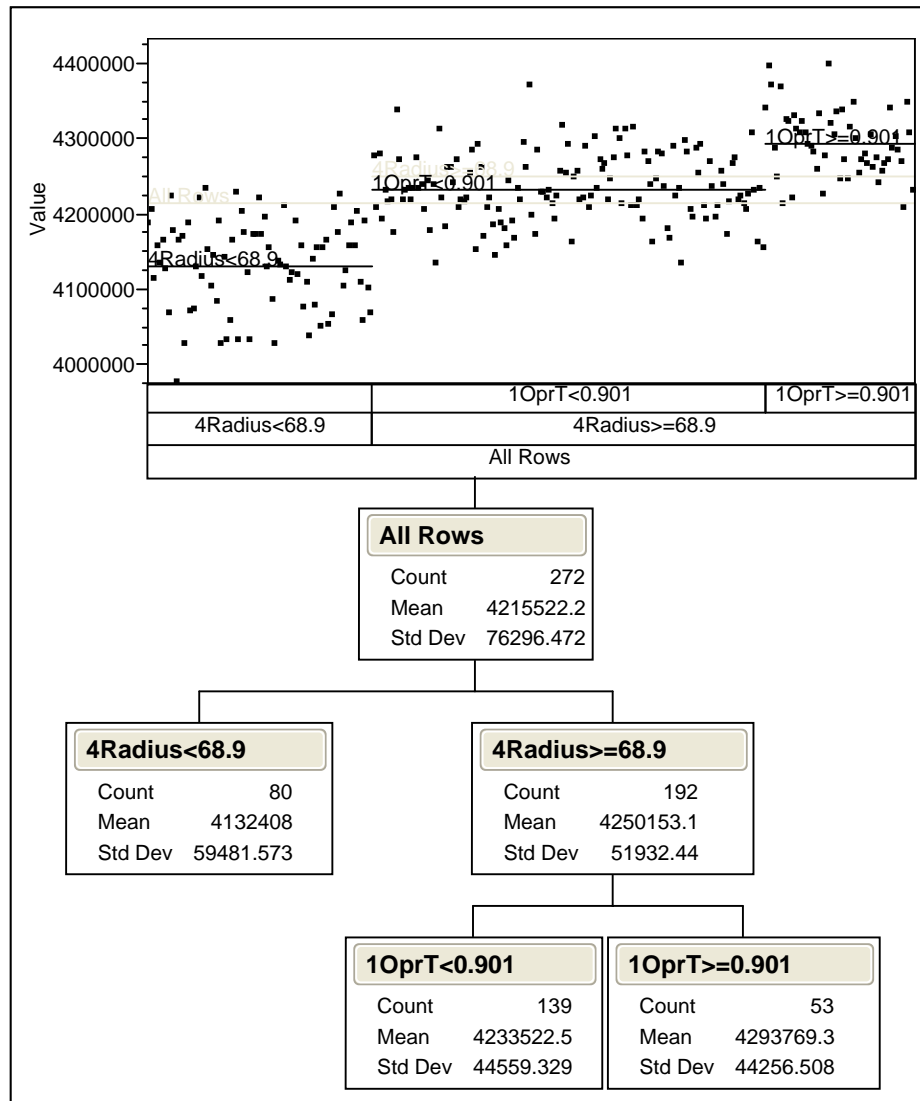
Figure 33.   Regression Tree for Mission Value Indicating the Significance of Class IV Operating Radius and Class I Operating Time.

From the regression analysis results, we observed the significance of the Class IV operating radius and Class I operating time. Additionally, the regression tree in Figure 33 provided an assessment in terms of the significant levels for each factor. Next, we produced a contour plot to demonstrate how the two factors affect the mission value together. Figure 34 displays the contour plot for Class IV operating radius vs. Class I operating time. Filled contour regions depict the mission value as the radius and operating time varies. Red regions in the lower edge of the plot indicate mission values less than or equal to 4.0×10^6. Blue and purple regions in the top and upper-right depict mission values greater than 4.3×10^6. The plot indicates that above average mission values can be achieved with a large range of settings as indicated in the region above line 1. We also get a better feel for the diminishing returns on increased Class IV operating radius as the Class I operating time is changed. Line 2 indicates the point at which substantial enhancements to mission value by Class IV operating radius begin to level-off. This effect varies across a wide range of Class I operating time mission values.
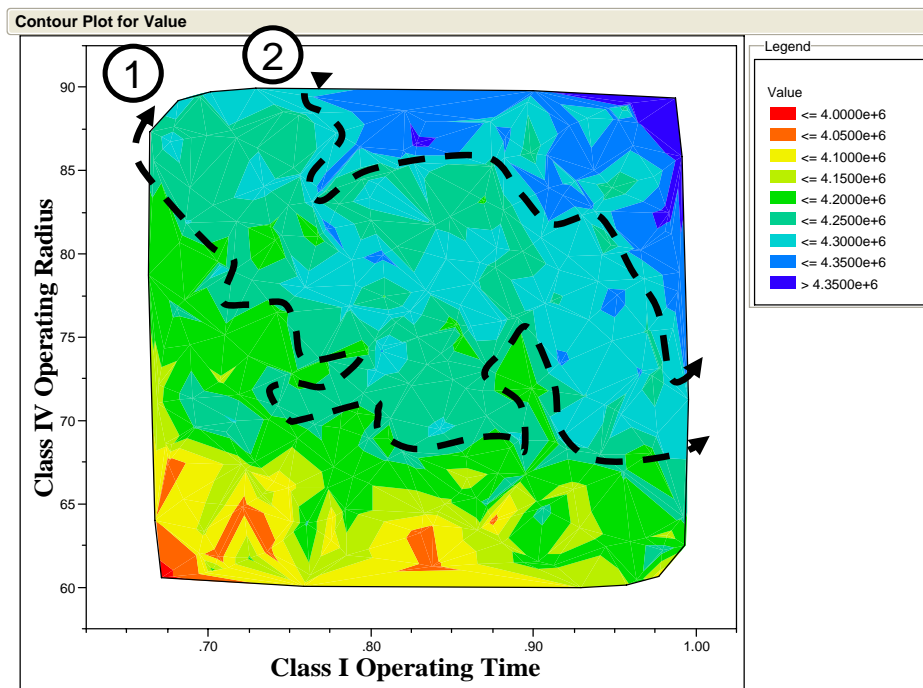
Figure 34.   Contour Plot for Mission Value with Class IV Operating Radius vs. Class I Operating Time.

72

The next section explores the significant interactions observed within the model. Our discussion makes use of interaction plots to investigate the effect between ERMP time horizon and operating time. The plots further highlight the diminishing return on mission value due to increased operating radius of Class IV aircraft.

6. Significant Interactions

Our final model for mission value contained one interaction term, ERMP time horizon with ERMP operating time. Recall from Chapter II that the Predator-based ERMP UAV is the largest of the five UAVs investigated in this study. It serves as a division level asset and is capable of serving all mission requirements except for SIGINT payloads. Significant findings and insights may assist in the development of employment considerations for this unmanned platform.

Figure 35 displays the profile plot indicating interaction between the two factors. In the plot, the y-axis represents the mission value. The smaller plots display the effect of two factors on the response. Solid lines indicate interaction between terms. There is one term listed on the diagonal plot for each column. The x-axis at the bottom of the graph represents the term's range. Changes in the term's value affect the mission value according to the slope of the lines found in the plots above and below the diagonal. The plots across each row display two lines, one each for the low and high values of the term listed in the diagonal for the given row. We can assess changes in the response variable when the row term is set to its low or high value and we vary the range of a term found in the columns to the left or right of the diagonal, holding all other effects constant.
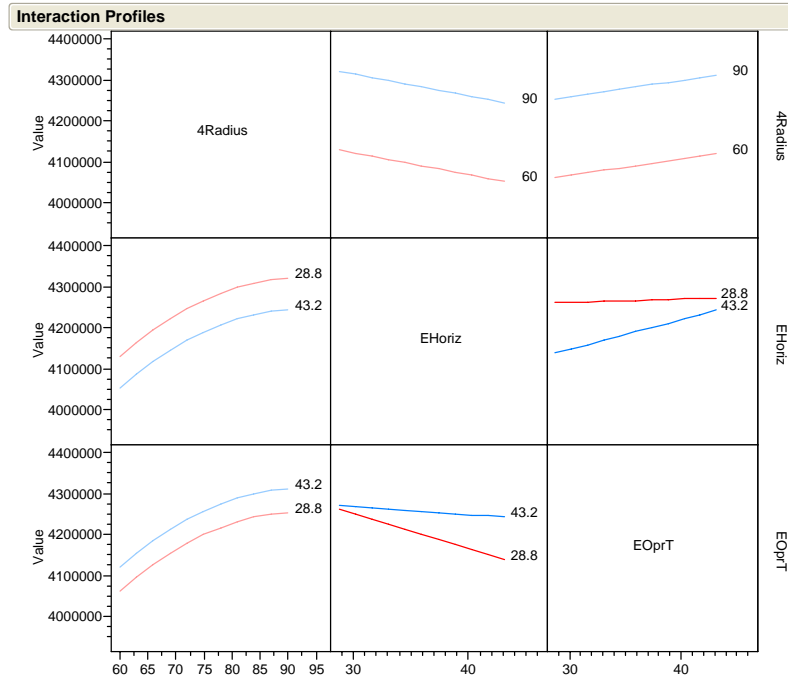
Figure 35.   Interaction Profile for Final Mission Value Model.

Looking at the middle row, we see ERMP time horizon crossed with ERMP operating time on the center-right plot. The top line represents the change to mission value when the time horizon is set at 28.8 hrs. The fact that this line is nearly flat with a slight positive slope indicates that there is only a small increase in mission value as the ERMP operating time increases across its entire range. However, when ERMP time horizon is set to its highest level of 43.2 hrs, mission value increases substantially as ERMP operating time increases. For our current range of values, the red line (top) represents the highest mission values when the horizon time is set to the ERMP UAV's lowest level of 28.8 km. This finding seems counterintuitive. It implies that when planning for ERMP UAV missions we should be myopic in our approach and consider a set of mission areas that become available sooner rather than a larger set of potential mission areas over a broader time window. Upon further investigation of the base scenario, we identified an explanation as to why the solution behaves in this manner.

The scenario examined in this study involves 21,360 mission requirements, of which 21,317 represent missions with a time window of 28.8 hrs or less. If the ERMP

74

time horizon is greater than 28.8, the optimization process attempts to allocate the UAV resource to missions of greater value within the extended future time horizon. In doing so, the process skips available missions of lesser value that are closer to the current simulation time. The cumulative and potentially larger value generated from serving multiple missions is lost. Additionally, when the ERMP time horizon is set to 28.8 hrs, the mission value increase only slightly as the operating time is increased. Based on the reasoning above, this result also makes sense. The lowest level for ERMP operating time is 28.8 hrs, identical to the platform's lowest level for time horizon. The UAV only requires 28.8 hrs to serve 99.8% of the missions within the scenario. Increases in its operating time may serve to increase its available loiter time on target. However, the increased loiter time is negligible due to the average mission length of 2.24 hrs for the 21,317 missions.

Additional insights gained from Figure 35 involve the combined effects of Class IV operating radius and ERMP time horizon. The center-top plot indicates that relatively high mission values are obtained when the Class IV operating radius is set at its maximum level of 90 km and ERMP time horizon is set at its lowest level of 28.8 hrs. However, we also observe a point of diminishing return for the effect of Class IV operating radius on mission value. The center-left plot on the interaction profile indicates this effect. When ERMP time horizon is set to its lowest level of 28.8 hrs, the effect of Class IV operating radius on mission value diminishes around 85 km, when all other effects remain constant. The contour plot in Figure 34 also suggests high mission values around this range. We observe that when Class I operating time is as low as 0.794 hrs and Class IV operating radius is around 86.5 km, the simulation generates the sixth highest mission value, increasing by 21% of its entire range.

The insights gained from exploring the interaction between ERMP time horizon and operating time, Class IV operating radius, and Class I operating time are significant. In the scenario examined by our study, the results indicate that overall mission success can be exploited by a relatively small ERMP time horizon and platform operating time. The next section develops an alternate regression model using percent mission coverage

as the response variable. We will discuss the development process, parameter estimates, and significant factors of the model.

D. PERCENT MISSION COVERAGE MODEL

The regression model developed for mission value provides an initial assessment to the solution of ASC-U. However, it is difficult to relate mission value to a tactical measure of effectiveness. This section describes the development of a regression model for the overall percent mission coverage for the scenario. We begin with some initial observations by reviewing the distribution of percent mission coverage and a scatterplot for the data. The section continues with a description of the final model and exploration of significant factors.

Figure 36 displays the distribution and summary statistics of percent mission coverage for all 272 designs. The base scenario design generated a percent mission coverage of 82.79%, slightly above the mean of 82.43%. A *Shapiro-Wilk* value of 0.99 at a significance of 0.97 indicates that a normal distribution fits the data well.
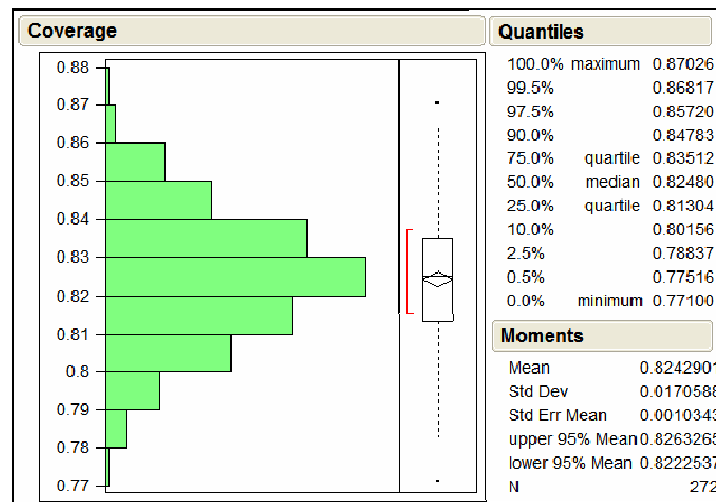
Figure 36.   Distribution and Summary Statistics of Percent Mission Coverage.

After reviewing the summary statistics, we generated the scatterplot for percent mission coverage in Figure 37. We observe similar extreme points as identified in Figure 21 for mission value. Interestingly, two design points, 21 and 22, replace 43 and 85 for fourth and fifth highest percent mission coverage values respectively. This finding indicates that mission value does not necessarily depict equivalent percent coverage. In the next section, we discuss the regression analysis that investigates these observations further.
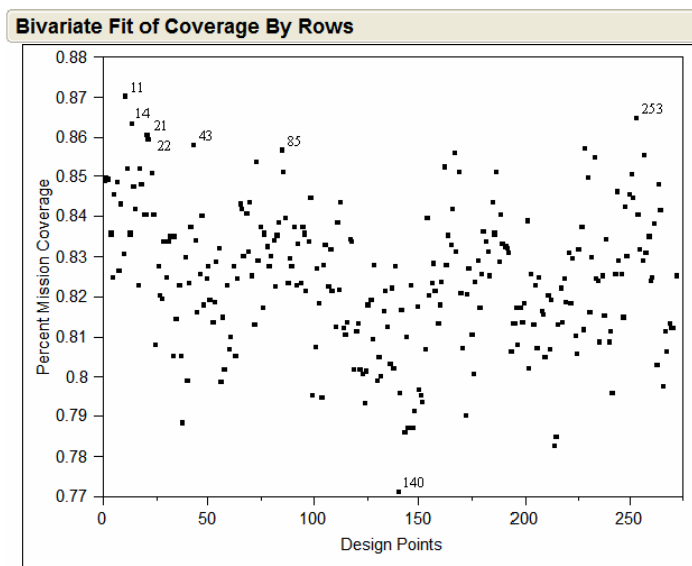
Figure 37.   Scatterplot of Percent Mission Coverage for Design Points.

1.   Final Model

Our analysis followed the same path as the development process for the mission value model described in Section C of this chapter. We explored the main effects, first order interactions, and second-order polynomial terms using stepwise mixed selection and standard least squares regression. We evaluated the history generated in the stepwise regression of the full quadratic model in order to construct a final model consisting of ten main effects and one second-order polynomial. The statistical report for the regression model for percent mission coverage is displayed in Appendix B. Table 11 displays the significant model terms and corresponding R-square values. Next, we evaluated the

terms using the *F* test. Table 12 displays the sequential *F* test for twenty-nine remaining terms from the full model. Based on the small *f*-statistic for the seventh term, we removed it from our final model. While terms 8 through 14 proved significant to the model, we decided to keep terms 8 through 12 in an attempt to avoid overfitting the model and maintain similar predictive power as our model for mission value.

Terms	Parameter	R-Square
1	1OprT	0.54420
2	4Radius	0.73984
3	1Radius	0.79817
4	EHoriz	0.83334
5	4Horiz	0.85283
6	3Horiz	0.86738
7	(3Horiz-6.00654)*(4Horiz-6.00434)	0.87000
8	EOprT	0.88547
9	3OprT	0.89683
10	(4Radius-75.0007)*(4Radius-75.0007)	0.90995
11	1Horiz	0.91762
12	4OprT	0.92464
13	3Radius	0.93162
14	1Speed	0.93574
15	2OprT	0.93809
16	(2OprT-1.99919)*(2OprT-1.99919)	0.94353
17	(EHoriz-35.9408)*(EOprT-35.9651)	0.94707
18	(3Horiz-6.00654)*(3OprT-5.98118)	0.95030
19	2Horiz	0.95144
20	ETrans	0.95145
21	(ETrans-0.49934)*(2Horiz-2.0036)	0.95289
22	(EOprT-35.9651)*(EOprT-35.9651)	0.95450
23	4Trans	0.95239
24	2Radius	0.95350
25	(3Radius-40.0978)*(3Radius-40.0978)	0.95514
26	4Speed	0.95591
27	(ETrans-0.49934)*(4Radius-75.0007)	0.95662
28	ESpeed	0.95698
29	(ESpeed-240.495)*(3OprT-5.98118)	0.95791

Table 11.   Significant Model Terms and Corresponding R-square Values for Percent
Mission Coverage Model.

	n =	272	numerator	denominator		$F_{a,k-l,n-(k+1)}$			
Terms	**SSE**	**df**	**df**	***f***	**0.0001**	**0.0010**	**0.0100**	**0.0500**
1	0.035946							
2	0.020517	1	269	202.28733	15.6003	11.0693	6.7300	3.8763
3	0.015917	1	268	77.44711	15.6021	11.0702	6.7304	3.8764
4	0.013143	1	267	56.34660	15.6039	11.0712	6.7307	3.8765
5	0.011606	1	266	35.22608	15.6057	11.0721	6.7311	3.8767
6	0.010459	1	265	29.08245	15.6075	11.0730	6.7315	3.8768
7	0.010252	1	264	5.31781	15.6093	11.0740	6.7318	3.8769
8	0.009032	1	263	35.52874	15.6111	11.0749	6.7322	3.8771
9	0.008136	1	262	28.85256	15.6130	11.0759	6.7326	3.8772
10	0.007102	1	261	38.01830	15.6149	11.0769	6.7330	3.8773
11	0.006496	1	260	24.21723	15.6167	11.0778	6.7334	3.8775
12	0.005943	1	259	24.12402	15.6186	11.0788	6.7337	3.8776
13	0.005392	1	258	26.33869	15.6205	11.0798	6.7341	3.8778
14	0.005067	1	257	16.48008	15.6225	11.0808	6.7345	3.8779
15	0.004882	1	256	9.72016	15.6244	11.0818	6.7349	3.8780
16	0.004453	1	255	24.57174	15.6264	11.0828	6.7353	3.8782
17	0.004174	1	254	16.95005	15.6283	11.0838	6.7357	3.8783
18	0.003920	1	253	16.43830	15.6303	11.0849	6.7361	3.8785
19	0.003830	1	252	5.91667	15.6323	11.0859	6.7365	3.8786
20	0.003829	1	251	0.06687	15.6343	11.0870	6.7369	3.8788
21	0.003755	1	250	4.91819	15.6364	11.0880	6.7373	3.8789
22	0.003667	1	249	5.96095	15.6384	11.0891	6.7378	3.8791
23	0.003538	1	248	9.08561	15.6405	11.0902	6.7382	3.8792
24	0.003477	1	247	4.31076	15.6426	11.0912	6.7386	3.8794
25	0.003421	1	246	4.03289	15.6447	11.0923	6.7390	3.8795
26	0.003393	1	245	2.03795	15.6468	11.0934	6.7394	3.8797
27	0.003320	1	244	5.36951	15.6489	11.0945	6.7399	3.8799
28	0.003231	1	243	6.62582	15.6511	11.0956	6.7403	3.8800
29	0.003164	1	242	5.14026	15.6533	11.0968	6.7408	3.8802

Table 12.   Model Utility *F*-test for Twenty-nine Terms Selected in the Stepwise Regression for Mission Percent Coverage.

Figure 38 displays the actual by predicted percent mission coverage plot for the final model. All of the factors were significant with a Prob>|t| <0.0001. The eleven terms account for 92% of the variance within the model. Two predictors accounted for nearly 74% of the variance within the model: Class I operating time at 54%, and Class IV operating radius for another 20%. This result was opposite that of the mission value model, which had Class IV operating radius accounting for 53% and Class I operating time for another 15%.
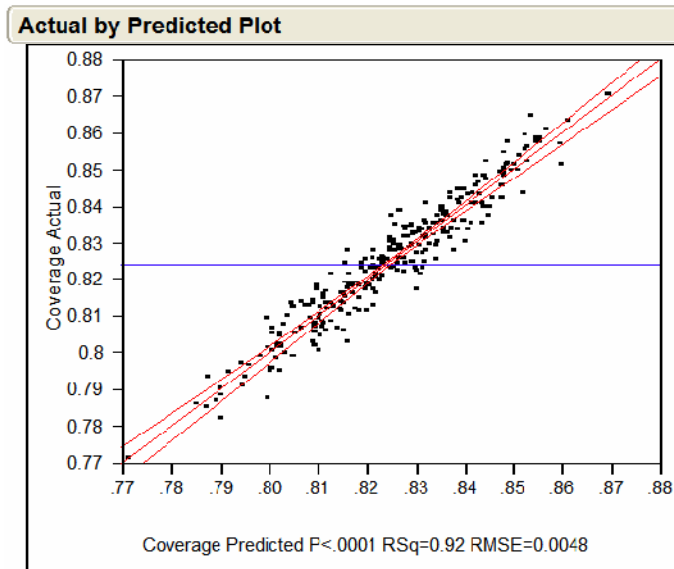
Figure 38.   Actual by Predicted Percent Mission Coverage Plot for Final Percent
Mission Coverage Model.
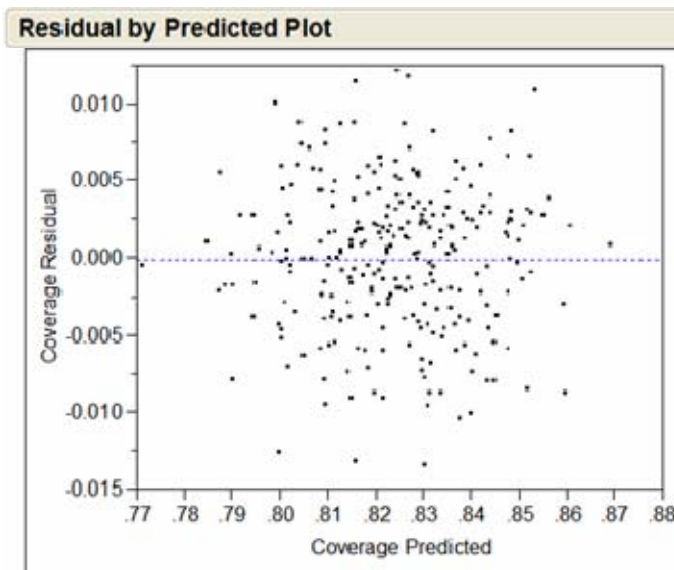
Figure 39.   Residual by Predicted Percent Mission Coverage Plot for Final Percent
Mission Coverage Model.

We observed the residuals in Figure 39 with an approximate mean of zero and random presentation, validating the assumption of homoscedasticity. Next, we checked the normality assumption with a histogram and Normal quantile plot of the residuals displayed in Figure 40. The plots along with a *Shapiro-Wilk* value of 0.99 at a significance of 0.26 indicates the residuals meet the Normality assumption.
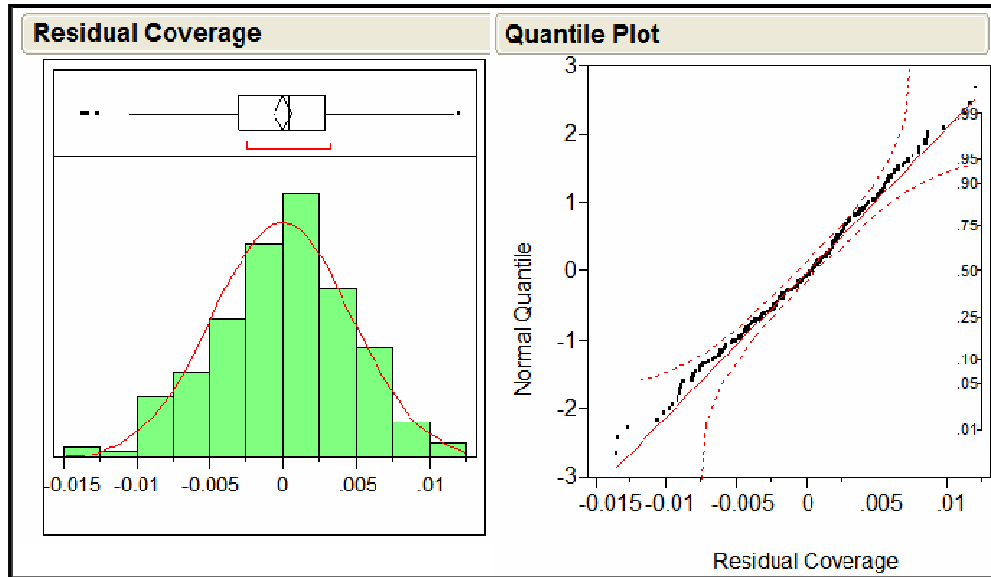
Figure 40.   Histogram and Normal Quantile Plot of Residuals for Final Percent Mission Coverage Model.

2.   Significant Factors

The percent mission coverage model contains a shift in significant factors compared to the mission value model developed in Section C. We see that the strength of the effect for Class I operating time and Class IV operating radius have reversed. As mentioned in the previous section, Class I operating time and Class IV operating radius explained 74% of the model. The Prediction Profiler in Figure 41 indicates that Class I operating time has the strongest effect on percent mission coverage. Class IV operating radius, Class I operating radius, and ERMP time horizon demonstrate a lesser effect. The remaining main effects display a relatively weak effect on percent coverage.
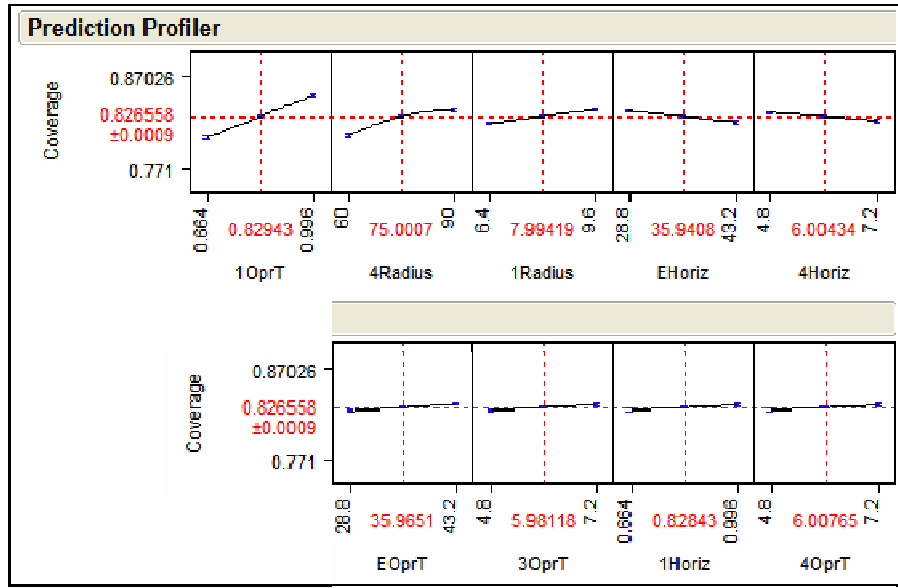
Figure 41. Prediction Profiler for Final Percent Mission Coverage Model.

As in the mission value model, ERMP time horizon demonstrates an inverse relationship with percent coverage. We also see this effect with Class IV time horizon. However, Class I time horizon matches our expectations of how the size of a "planning window" should effect the overall mission coverage for a scenario. We can explain the "myopic" behavior for Class IV UAVs in a similar fashion as we did for ERMP UAVs in Section C.6. We ran the experiments with the Class IV time horizon set at 4.8 to 7.2 hrs. Ninety-four percent of the missions within the scenario have a length of 4.8 hours or less. We suspect that the UAV could complete many of these missions prior to other valuable missions becoming available in the future. Further support for this concept is the fact that the average mission length is 2.24 hrs for 99.8% of the missions. As the time horizon increases, the simulation attempts to allocate Class IV UAVs to missions that are more valuable in the future. The result is the potential loss of missions that occur sooner and hence the loss of mission coverage due to a cumulative effect.

We explain the direct relationship of Class I time horizon to percent mission coverage in a different way. We ran the experiments with the Class I time horizon set at 0.664 to 0.996 hrs. The optimization interval is set to occur every hour. The simulation

is only able to allocate UAVs to missions "seen" within the time window for Class I platforms. This results in the simulation not being able to "see" missions that occur beyond the time of the next optimization sequence. Therefore, Class I UAVs are assigned to missions that are available at the time of the optimization sequence and up to a fraction of the time (0.664-0.996) until the next optimization. Since the Class I also varies its operating time between 0.664 and 0.996 hrs and its transition time between 0.128 and 0.192 hrs, Class I UAVs that launch and serve mission areas at each optimization interval may not be available for higher value missions during the next optimization sequence. The Class I UAV is unique; it is the only platform with horizon and operating times less than the optimization interval of one. We suspect that increasing the horizon and operating time ranges for Class I platforms may yield interesting results, to include curvilinear effects where we see a point of diminishing returns or inverse effects on percent mission coverage.

Figure 42 displays the regression tree for percent mission coverage after the first five splits. In the first split, the tree indicates that when Class I aircraft have an operating time of greater than or equal to 0.787 hrs, the overall percent coverage tends to be higher. While this only results in a one percent increase to the mean percent coverage, it represents nearly an eight percent increase over the range of the results for this MOE. Class I operating time generates the second split, increasing the mean by another percent at operating times greater than or equal to 0.905 hrs. The third split falls under Class I operating time of less than 0.787 hrs and occurs when Class IV operating radius is delineated above and below 69.0 km. The fourth split occurs when Class I operating time is between 0.787 and 0.905 hrs. The significant factor in this split is Class IV operating radius, and results in an overall mean of 82.94% for percent coverage. The final split is displayed on the right-hand side of the figure. It is represented by Class IV operating radius >= 69.1 km and falls under Class I operating times >= 0.905 hrs. The result is a two percent increase to the percent coverage of the baseline scenario, which corresponds to twenty percent of the observed range of the MOE.
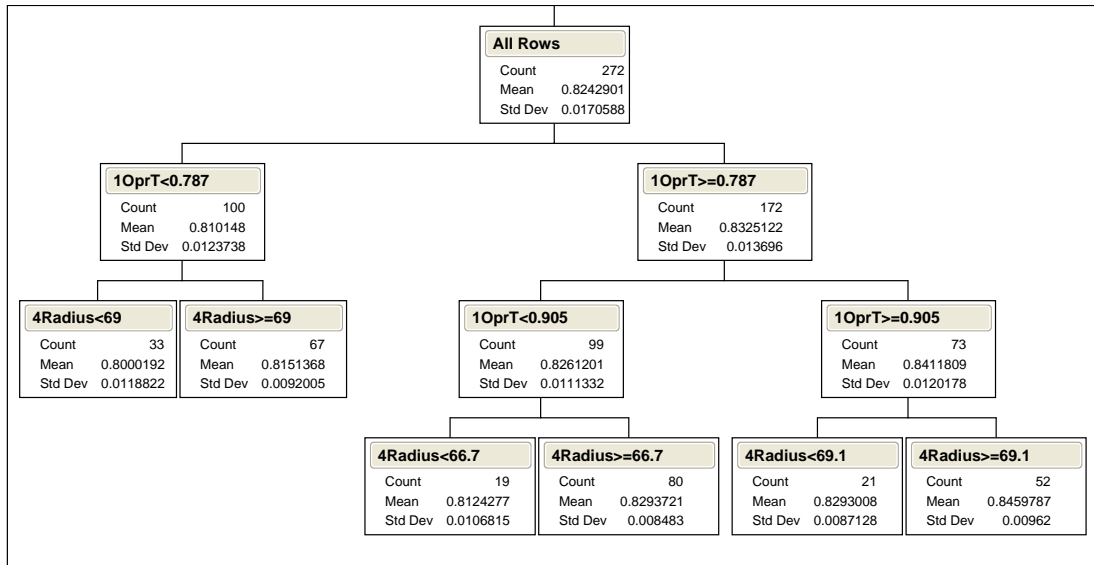
Figure 42.   Regression Tree for Percent Mission Coverage Indicating the Significance of Class I Operating Time and Class IV Operating Radius.

As in the mission value model, we produced a contour plot to demonstrate how Class I operating time and Class IV operating radius relate together with their effect on percent mission coverage. Figure 43 displays the contour plot for Class IV operating radius vs. Class I operating time. Filled contour regions depict the percent mission coverage as the two factors vary. The region to the right of the first line on the left indicates percent mission coverage at or above eighty percent. We point out that such results occur when both factors are set below the base scenario settings. This result may be of interest when assessing platform requirements in future studies. Regions to the right of the second line indicate percent coverage at or above 83.7%. Here we see a trade-off required for the factors such that when one UAV is operating at or below its base scenario setting, the other must operate at levels above the base setting. However, in the case of the Class I operating time, this amounts to only a few minutes as noted in Section C.5 of this chapter.
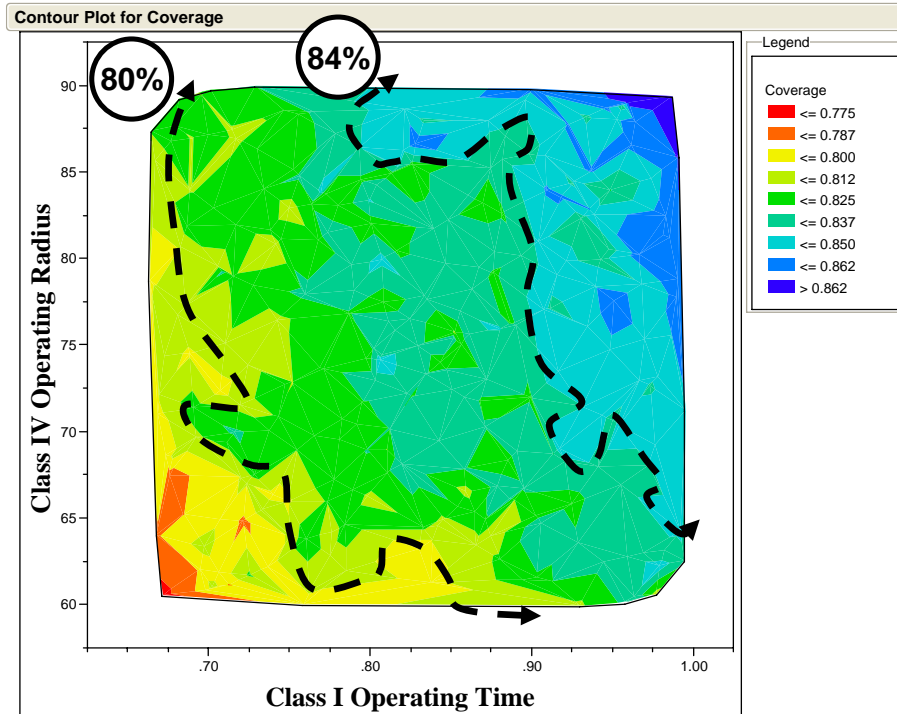
Figure 43.   Contour Plot for Percent Mission Coverage with Class IV Operating
Radius vs. Class I Operating Time.

E.   INTERESTING OBSERVATIONS

This section describes several interesting observations identified during our analysis. We begin with a comparison of the two measures of effectiveness used in our regression models. Additionally, we discuss the most significant factor effects for each measure of effectiveness generated by the ASC-U version investigated in our study. Next, we use a parallel plot to highlight the importance of reviewing more than one or two MOEs. Finally, we interpret the signs on the model coefficients.

1.   Measure of Effectiveness Comparison

We developed two regression models using mission value and percent mission coverage. Our intent was to investigate how the UAV performance characteristics influenced ASC-U's solution. After conducting regression analysis for our mission value model, we realized it was difficult to get a tactical sense of the MOE. Upon conducting regression analysis for percent mission coverage, we immediately recognized a difference

in the two measures based on their opposing significant factors. The switch between Class IV operating radius and Class I operating time demonstrates a fundamental difference between the two.

Initially, mission value and percent mission coverage seem to imply a similar measure of effectiveness. Recall from Chapter II that mission value is derived from a value rate that is dependent on the mission area and required sensor package. This "weighting" system may result in a scenario with a mission value that does not correspond to an equivalent percent mission coverage. For example, mission areas with more valuable sensor package requirements may be served in such a way to limit multiple servicing of other mission areas. The cumulative effect results in a high mission value, but relatively low percent mission coverage.

Figure 44 displays the difference between the two measures by mapping the combined 514 runs from our initial and final DOEs. The green plot represents the 257 design points from the initial DOE where we varied the optimization interval from one to ten simulation hours. The blue plot represents our final DOE where optimization interval remained fixed at one simulation hour. The red plots indicate the corresponding percent mission coverage for each design point. Notice that mission value is "over representative" of the overall percent coverage across most of the initial design. However, the mission values are more representative of the percent coverages in the final design. We believe that the larger optimization intervals drive the allocation of UAV assets to high value areas and reduce the cumulative effect of covering more missions when optimization intervals are small.

After exploring the MOEs used in our two regression models, we turned our attention towards the significant factors that affect a change in the mean value generated by our design runs for each MOE. We employed JMP's partitioning platform in order to identify the regressor involved in the first split against each MOE as the response variable. The results identified the factor responsible for the optimum split, separating the response variable into two groups of different means. We identified the significant factor, the level of the factor identifying the branch with the increased mean, the percent

increase over the range of the examined MOE, and the percent increase in coverage (except in the case of mission value). Table 13 displays the results of the exploration.
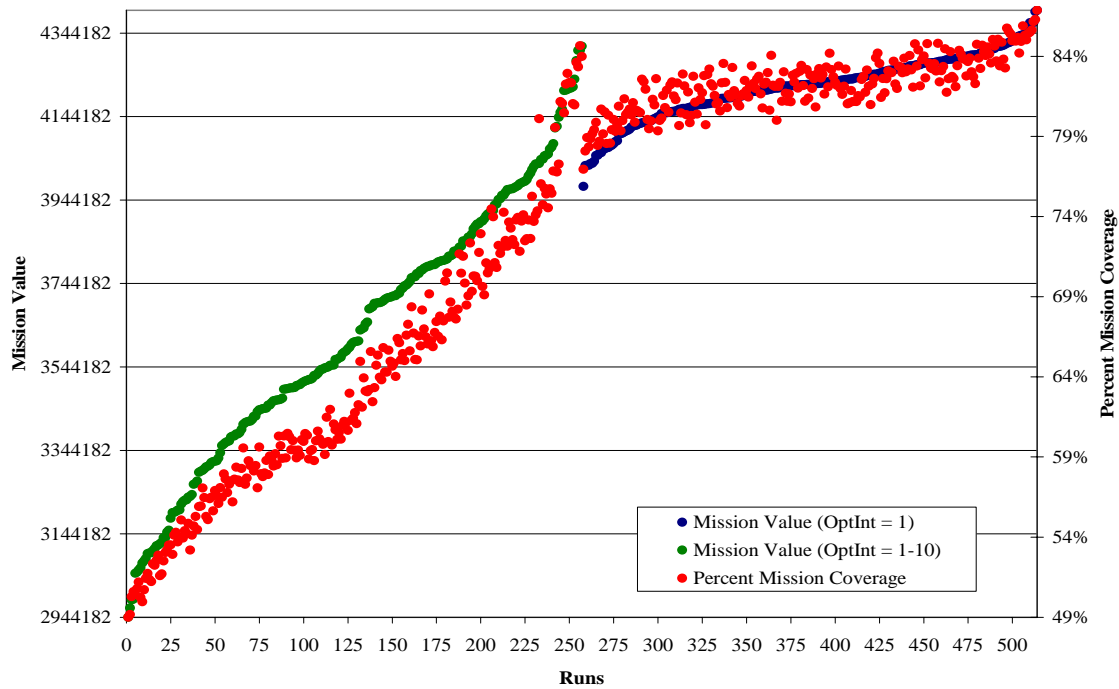
Figure 44.   Comparison of Mission Value and Percent Mission Coverage for Initial and Final Design of Experiments.

The most significant increase in percent coverage occurred for the meteorological sensor package at 15.12% increase to the mean when Class III operating radius is set at greater than or equal to 41.9 km. This result corresponds to a 30.24% increase over the entire range of percent coverage for meteorological missions. While the other splits did not cause a substantial increase to the mean of the other MOEs, we note that five splits resulted in a 15% or greater increase over the range of the MOE studied. Class IV operating radius and Class I operating time with seven splits each represented the largest number of splits for the twenty-one MOEs. Class III operating radius produced one split. It was the most significant factor to influence the mean of meteorological percent coverage. Interestingly, Class I operating time was the most significant factor for percent coverage by type of all the UAVs. Finally, supply delivery missions were never allocated

UAVs. While this is interesting, there were only five such missions in the entire scenario.

MOE (Response)	Significant Factor (First Split)	Base Scenario Setting	Partition Value Creating Positive Increase on Mean	Percent Increase over Range of MOE	Percent Increase in Coverage
Value	4Radius	75 km	>= 68.9 km	8.21%	
Percent Coverage	1OprT	0.830 hrs	>= 0.787 hr	8.28%	0.82%
Supply Delivery					
Meterological	3Radius	40 km	>= 41.9 km	30.24%	15.12%
COMINT	4Radius	75 km	>= 68.9 km	19.59%	6.60%
Weapon	EOprT	36 hrs	>= 38.8 hr	15.54%	3.33%
ELINT	4Radius	75 km	>= 68.9 km	15.43%	3.82%
Class II UAV	1OprT	0.830 hrs	>= 0.816 hr	14.36%	0.50%
Clas III UAV	1OprT	0.830 hrs	>= 0.894 hr	13.00%	0.57%
Class I UAV	1OprT	0.830 hrs	>= 0.816 hr	11.31%	1.06%
Class IV UAV	1OprT	0.830 hrs	>= 0.789 hr	10.38%	0.21%
ERMP	1OprT	0.830 hrs	>= 0.787 hr	7.35%	0.16%
GPS Designator	EHoriz	36 hrs	< 30.7 hr	29.16%	6.11%
Laser Designator	4Radius	75 km	>= 77.6 km	15.01%	1.70%
EO/IR/LR	1OprT	0.830 hrs	>= 0.770 hr	9.41%	1.02%
SAR/MTI	4Radius	75 km	>= 67.6 km	7.29%	0.65%
Comms Relay	EHoriz	36 hrs	< 36.7 hr	6.85%	0.60%
EW	EOprT	36 hrs	>= 32.3 hr	6.35%	1.37%
Mine Detection	4Radius	75 km	>= 66.2 km	5.90%	0.61%
CBRNE	4Radius	75 km	>= 64.2 km	5.27%	1.47%
FOPEN/LIDAR	EOprT	36 hrs	< 42.9 hr	1.63%	0.03%

Table 13. First Split on Partition of MOEs Indicating Significant Factor and Percent Increase over Range of MOE and Percent Increase in MOE Coverage.

Figure 45 displays a parallel plot to highlight the importance of reviewing more than one or two MOEs. The plot allows us to explore the relative results of all of the MOEs simultaneously. We have selected the six design points that resulted in extreme values as previously noted in Figure 24 (points 11, 14, 43, 85, and 253 in green and point 140 in red). We note that while the design points in green represent the highest mission values within our DOE, they result in some of the lowest percent coverages for numerous MOEs. Regions 1 and 2 emphasize this fact by indicating where designs 85 and 253 are separated from designs 11, 14, and 43 within the bimodal distribution of meteorological percent coverage (Meteo). Additionally, we observe design point 43 representing one of the lowest outcomes for FOPEN/LIDAR percent coverage (FOPEN) in region 4. Alternatively, design point 140 resulted in the lowest mission value out of 272 runs. However, it does not represent the lowest percent coverage for several MOEs. This is

evident in region 3 for FOPEN coverage. Again, we point out that all design points resulted in 0 percent coverage for supply delivery (Supply), as indicated in region 5.

The next section provides an interpretation of the signs on the model coefficients. As previously noted in the chapter, the time horizon factor influenced the response variable counter to our expectations for four of the five UAVs. We discuss additional factors that have opposite signs than predicted.

2. Interpretation of Model Coefficients

We had expectations on how UAV performance capabilities would influence the solution generated by ASC-U. However, several of the signs on the coefficients within the models are counterintuitive. Table 14 provides a comparison between our predicted coefficient signs and the actual signs generated within the regression models for each UAV type. Factors with counterintuitive signs are highlighted in yellow and bold type. It is important to note that the difference between the signs is not due to multicollinearity between the regressors; our design methodology eliminates this as a possibility. In addition to reviewing the pairwise correlations between the factors of our design matrix (see Chapter IV, Section B.2), we also examined the variance inflation factors (VIF) between regressors within our final models. The magnitude of the VIF serves as an important multicollinearity diagnostic. The minimum and maximum VIF values within our models were 1.00 and 1.01, respectively. VIF values greater than 5 indicate serious multicollinearity problems between regressors (Montgomery et al., 2001).

In Table 14, we see that all of the time horizons have a negative slope except for Class I UAVs. We provided our interpretation of the counterintuitive signs for ERMP, Class I, and Class IV UAVs in Sections C.6 and D.2 of this chapter. We offer the same explanation for Class II and III UAVs. We contend that the UAVs with greater range and endurance seek out higher value missions and miss the cumulative effect of serving several "closer-in" missions. On the other hand, Class I UAVs are the only type of UAV with time horizon interval less than one simulation hour. They simply do not have the "opportunity" to compare additional missions.
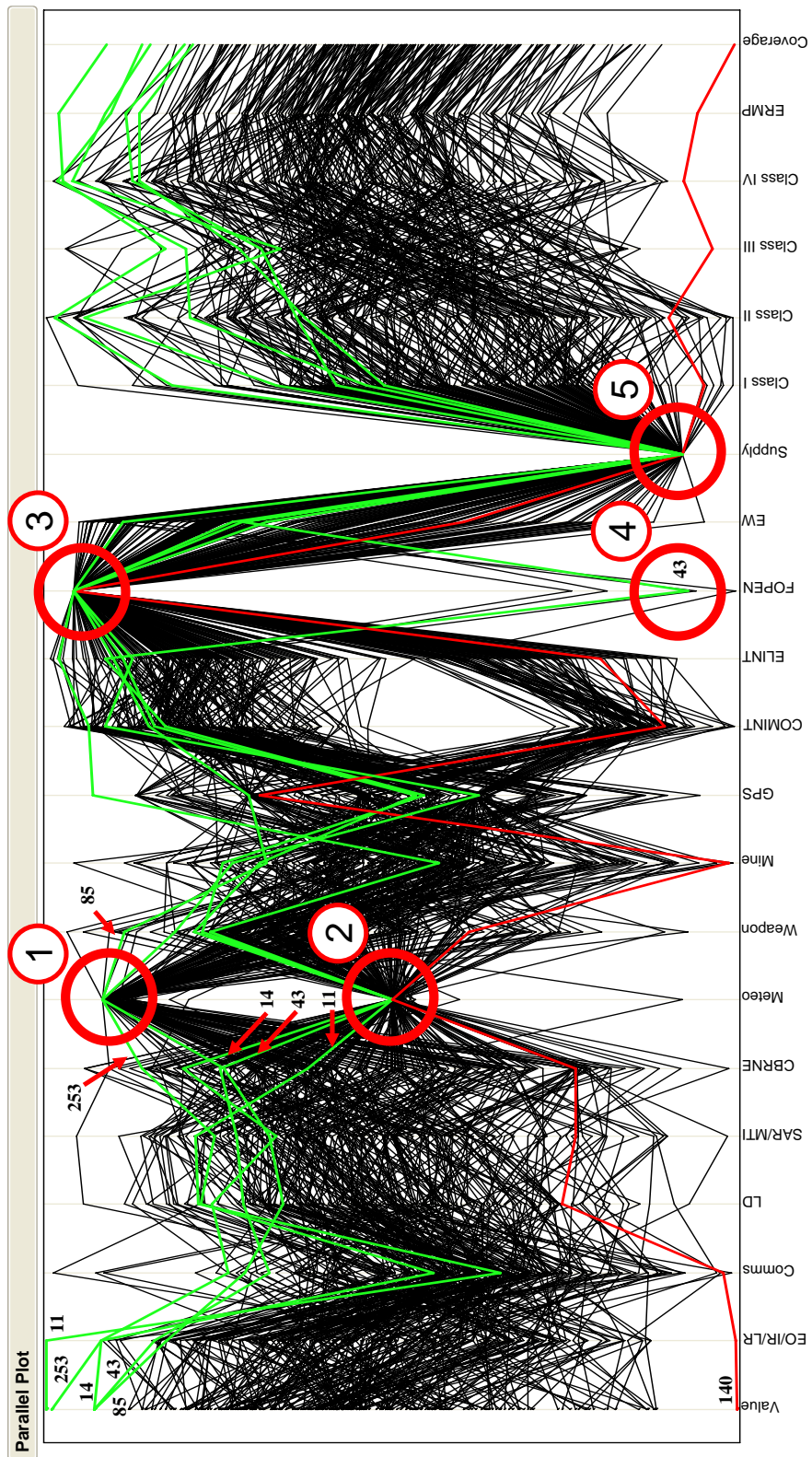
Figure 45.   Parallel Plot Displaying Corresponding Results for MOEs.

Table 14 also displays additional, counterintuitive signs for the coefficients of the ERMP UAV's operating radius and the Class II UAV's operating and transition times. The slopes suggest that smaller ERMP operating radii and Class II operating times, as well as longer Class II transition times increase mission value and percent mission coverages. While these regressors are not found in the final models for mission value or percent mission coverage, they are consistently represented in this way throughout our exploratory regression analysis as we constructed our final models. We do not provide an in-depth analysis of these counterintuitive results, except to note that their VIF values fall within the range described above. We recommend further analysis to identify the processes within the simulation model that account for these unique results.

UAV Types	Factors	Predicted Sign on Coefficient	Actual Sign on Coefficient
ERMP			
	Time Horizon (hr)	+	-
	Operating Time (hr)	+	+
	Air Speed (km/hr)	+	+
	Operating Radius (km)	+	-
	Transition Time (hr)	-	-
Class I			
	Time Horizon (hr)	+	+
	Operating Time (hr)	+	+
	Air Speed (km/hr)	+	+
	Operating Radius (km)	+	+
	Transition Time (hr)	-	-
Class II			
	Time Horizon (hr)	+	-
	Operating Time (hr)	+	-
	Air Speed (km/hr)	+	+
	Operating Radius (km)	+	+
	Transition Time (hr)	-	+
Class III			
	Time Horizon (hr)	+	-
	Operating Time (hr)	+	+
	Air Speed (km/hr)	+	+
	Operating Radius (km)	+	+
	Transition Time (hr)	-	-
Class IV			
	Time Horizon (hr)	+	-
	Operating Time (hr)	+	+
	Air Speed (km/hr)	+	+
	Operating Radius (km)	+	+
	Transition Time (hr)	-	-

Table 14.   Comparison of Predicted and Actual Coefficient Signs.

THIS PAGE INTENTIONALLY LEFT BLANK

VI.   CONCLUSIONS

If the Division Commanders want a UAV at their level and have nothing now, we ought to give it to them.

LTG Scott Wallace, CG V Corps (2003)
(Sinclair, 2005)

The U.S. Army Training and Doctrine Command (TRADOC) Analysis Center (TRAC) and the Modeling, Virtual Environments, and Simulations Institute (MOVES) at the Naval Postgraduate School, Monterey, California developed the Assignment Scheduling Capability for UAVs (ASC-U) simulation tool to assist in the analysis of UAV requirements. TRAC selected ASC-U for the Army-wide UAV Mix Analysis that supports investment strategies involving technology for current operations, transitioning to modular forces, and developing and fielding the Future Combat Systems (FCS) (Witsken, 2004). This thesis has explored the effects of twenty-six simulation and UAV factors on the Measures of Effectiveness (MOE) generated by ASC-U.

We combined data analysis, exploratory modeling and a Nearly Orthogonal Latin Hypercube design to examine 514 design points. In doing so, we expanded the use of ASC-U from running single scenarios with baseline settings to a full exploration process across multiple factors. The application and insights gained will support current and future warfighters. The conclusions suggest the following:

- The optimization interval significantly influences the solution.
- Mission value and percent mission coverage are not equivalent MOEs.
- Optimization interval of one simulation hour provides better correlation between mission value and percent mission coverage.
- Each measure of effectiveness has a different set of significant factors.
- Counterintuitive time horizon coefficients highlight models' allocation process.
- Class I operating time and Class IV operating radius are main factors influencing 14 of 21 MOEs.

- Class IV operating radius begins to make significant improvement to percent mission coverage at below baseline settings.
- Longer Class I operating times increase all other UAV mission percent coverages.
- State-of-the-art Design of Experiment and data mining techniques yield insights impossible to gain otherwise.

A.   IMMEDIATE IMPACT

The Army Chief of Staff tasked TRADOC to evaluate the current, modular, and Future Combat Systems (FCS) force options with regard to UAVs and develop an investment strategy. The analysis supports the development of an acquisition strategy for UAVs at the Division and Brigade level. Additionally, the analysis assists in defining the near term (2008) UAV force structure and the investment strategy for the mid term (2013), and far term (2018).

This thesis addresses the directives of TRAC by providing an analysis of the time horizon and optimization interval used in ASC-U's optimization process, UAV performance characteristics, and the appropriate design of experiment tools used in the Army UAV Mix Analysis.

B.   FOLLOW ON RESEARCH

This thesis blended different techniques involving simulation, optimization, and state-of-the-art design of experiments to achieve substantial insights regarding the allocation of UAVs within an advanced assignment and scheduling simulation. While we made significant advancement in combining DOE and data mining techniques with the simulation, we suggest the following list for future research:
- Continue integration of DOE tools with the simulation interface.
- Study additional scenarios developed by TRAC.
- Explore effects of optimization interval at levels below one simulation hour.
- More rigorously determine the range of factors through the acquisition community.
- Study trade-offs between UAV capabilities in more detail.

- Explore number and type of UAVs at different echelons.

- Expand simulation to account for attrition and maintainability.

- Expand factor ranges to explore possible curvilinear effects.

- Investigate MOEs displaying bimodal distributions.

- Conduct cost analysis on UAV performance characteristics in relation to the measures of effectiveness generated by the simulation.

- Establish parameters representing mission area densities and study their effects on the simulation's solution.

THIS PAGE INTENTIONALLY LEFT BLANK

APPENDIX A.   MISSION VALUE MODEL

The figure below displays the statistical report for the final regression model for mission value.

Response Value

Summary of Fit

RSquare	0.920978
RSquare Adj	0.917635
Root Mean Square Error	21896.57
Mean of Response	4215522
Observations (or Sum Wgts)	272

Analysis of Variance

Source	DF	Sum of Squares	Mean Square	F Ratio
Model	11	1.45287e12	1.3208e11	275.4752
Error	260	1.2466e+11	479459863	Prob > F
C. Total	271	1.57753e12		<.0001

Parameter Estimates

Term	Estimate	Std Error	t Ratio	Prob>|t|	VIF
Intercept	3446141.8	34710.67	99.28	<.0001	.
4Radius	6397.9899	153.1702	41.77	<.0001	1.0019602
1OprT	311592.55	13916.5	22.39	<.0001	1.0009492
EHoriz	-5344.016	317.8051	-16.82	<.0001	1.0016585
EOprT	3984.088	321.3805	12.40	<.0001	1.001416
(EHoriz-35.9408)*(EOprT-35.9651)	451.24159	73.36855	6.15	<.0001	1.0115686
3Radius	2348.7894	286.3274	8.20	<.0001	1.0019254
1Radius	11080.025	1428.815	7.75	<.0001	1.0023671
(4Radius-75.0007)*(4Radius-75.0007)	-186.175	19.99839	-9.31	<.0001	1.0109111
4Horiz	-12354.99	1902.569	-6.49	<.0001	1.0006291
3Horiz	-10686.6	1892.326	-5.65	<.0001	1.002233
4OprT	8232.1434	1923.914	4.28	<.0001	1.0008135

Effect Tests

| Source	Nparm	DF	Sum of Squares	F Ratio	Prob > F
4Radius	1	1	8.36548e11	1744.773	<.0001
1OprT	1	1	2.40362e11	501.3189	<.0001
EHoriz	1	1	1.35571e11	282.7573	<.0001
EOprT	1	1	7.36836e10	153.6805	<.0001
EHoriz*EOprT	1	1	1.81364e10	37.8267	<.0001
3Radius	1	1	3.22637e10	67.2918	<.0001
1Radius	1	1	2.88325e10	60.1353	<.0001
4Radius*4Radius	1	1	4.15532e10	86.6667	<.0001
4Horiz	1	1	2.02189e10	42.1701	<.0001
3Horiz	1	1	1.52911e10	31.8924	<.0001
4OprT	1	1	8778224640	18.3086	<.0001

THIS PAGE INTENTIONALLY LEFT BLANK

APPENDIX B. PERCENT MISSION COVERAGE MODEL

The figure below displays the statistical report for the final regression model for percent mission coverage.

Response Coverage

Summary of Fit

RSquare	0.92276
RSquare Adj	0.919492
Root Mean Square Error	0.00484
Mean of Response	0.82429
Observations (or Sum Wgts)	272

Analysis of Variance

Source	DF	Sum of Squares	Mean Square	F Ratio
Model	11	0.07277061	0.006616	282.3741
Error	260	0.00609133	0.000023	Prob > F
C. Total	271	0.07886194		<.0001

Parameter Estimates

Term	Estimate	Std Error	t Ratio	Prob>|t|	VIF
Intercept	0.6235384	0.007959	78.35	<.0001	.
1OprT	0.1321763	0.003076	42.97	<.0001	1.0009701
4Radius	0.0008755	0.000034	25.86	<.0001	1.0019702
1Radius	0.0044126	0.000316	13.97	<.0001	1.0026656
EHoriz	-0.000768	0.00007	-10.94	<.0001	1.000451
4Horiz	-0.003395	0.000421	-8.07	<.0001	1.0013319
3Horiz	-0.003028	0.000418	-7.24	<.0001	1.0019146
EOprT	0.0004955	0.000071	6.97	<.0001	1.0019149
3OprT	0.0025562	0.000425	6.02	<.0001	1.0015039
(4Radius-75.0007)*(4Radius-75.0007)	-0.00003	0.000004	-6.85	<.0001	1.0010327
1Horiz	0.0158068	0.003048	5.19	<.0001	1.0020744
4OprT	0.0020678	0.000425	4.86	<.0001	1.0006069

Effect Tests

Source	Nparm	DF	Sum of Squares	F Ratio	Prob > F
1OprT	1	1	0.04325044	1846.087	<.0001
4Radius	1	1	0.01566462	668.6231	<.0001
1Radius	1	1	0.00457151	195.1287	<.0001
EHoriz	1	1	0.00280461	119.7112	<.0001
4Horiz	1	1	0.00152551	65.1141	<.0001
3Horiz	1	1	0.00122784	52.4088	<.0001
EOprT	1	1	0.00113923	48.6264	<.0001
3OprT	1	1	0.00084818	36.2032	<.0001
4Radius*4Radius	1	1	0.00109872	46.8975	<.0001
1Horiz	1	1	0.00063023	26.9005	<.0001
4OprT	1	1	0.00055399	23.6465	<.0001

THIS PAGE INTENTIONALLY LEFT BLANK

APPENDIX C.   METEOROLOGICAL REGRESSION TREE
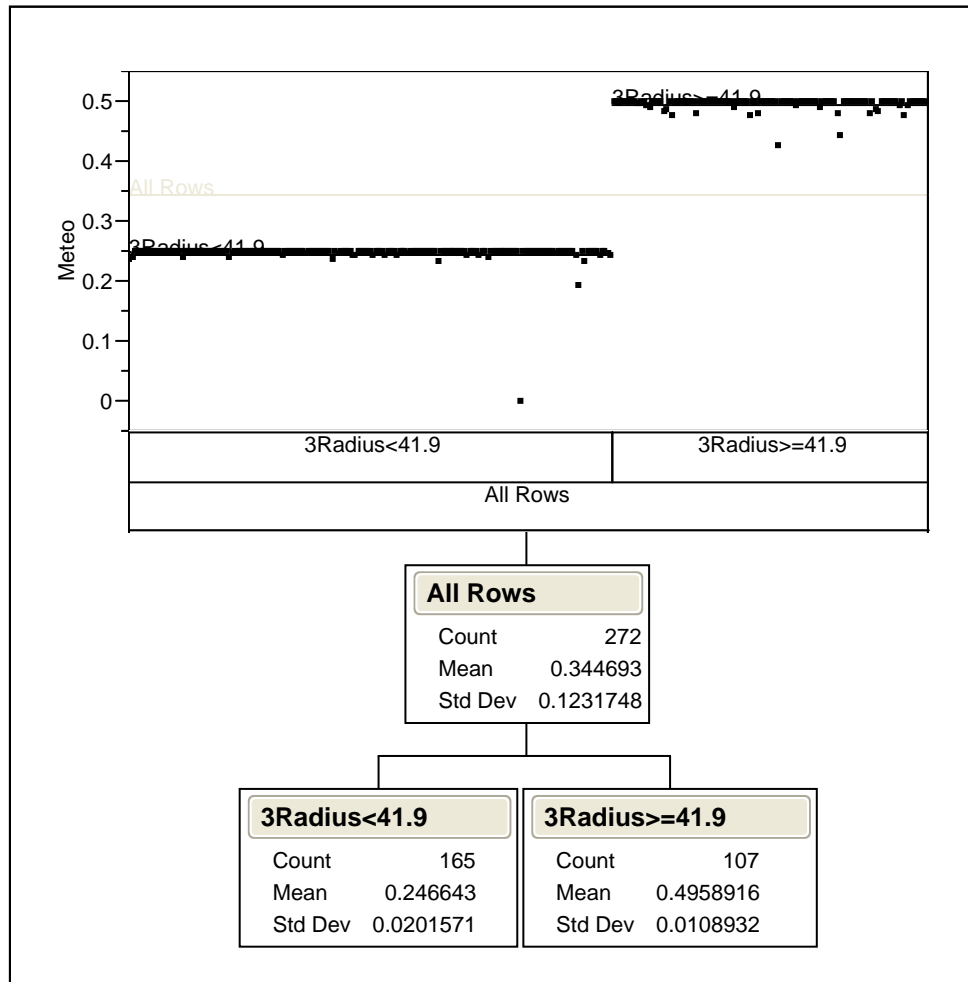
The regression tree above indicates that when Class III aircraft have an operating radius of greater than or equal to 41.9 km, the mean percent coverage for meteorological missions is increased by 16% for the scenario used in this study. This also corresponds to nearly a 200% increase to the meteorological percent coverage of the baseline scenario.

THIS PAGE INTENTIONALLY LEFT BLANK

APPENDIX D.   COMINT REGRESSION TREE
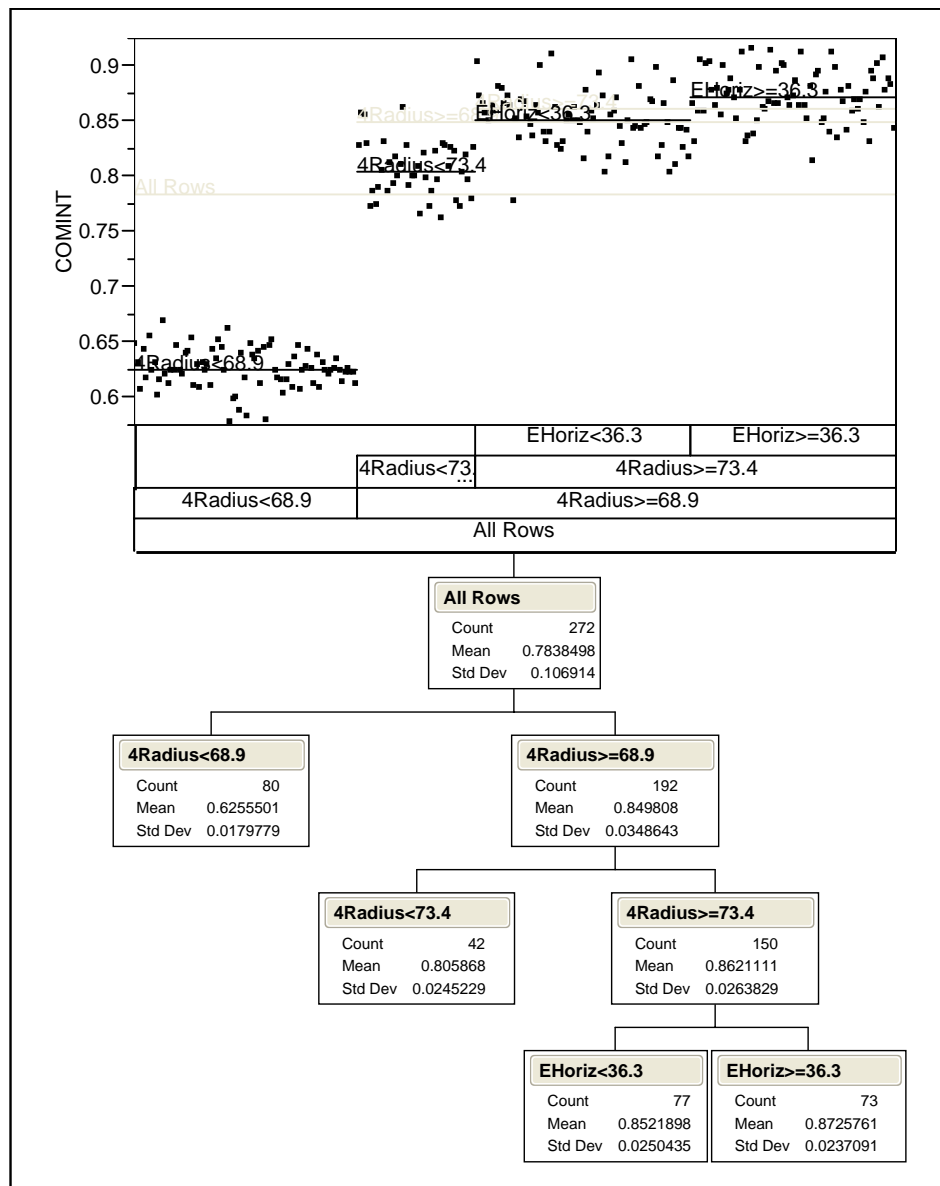
The regression tree above displays the first three splits for COMINT percent coverage. The third split on the right is represented by ERMP time horizon >= 36.3 hrs and falls under Class IV operating radius >= 73.4 km. The result is a two percent increase to COMINT percent coverage of the baseline scenario. This corresponds to nine percent of the variation of the MOE.

THIS PAGE INTENTIONALLY LEFT BLANK

APPENDIX E.   JAVA CODE FOR DATA CONSOLIDATION

The Java™ code within this appendix calculates percent mission coverage by UAV type and consolidates the results. Microsoft® Visual Basic® macros were also created in order to generated ASC-U input files, calculate MOEs and consolidate the results. The author will provide additional code upon request.

```java
/*
 * File: CoverageByType.java
 * Created on May 1, 2006, 11:34 PM
 */

/**
 * @author Christopher J. Nannini
 * Class to Consolidate Percent Coverage by UAV for 257 Design Points
 * from ASC-U Write-Output Microsoft Access Database.
 */

package ascuManager;
import java.sql.Statement;
import java.sql.Connection;
import java.sql.DriverManager;
import java.sql.ResultSet;
import java.text.DecimalFormat;

public class CoverageByType {

    public static void main(String[] args) {
        DecimalFormat numberFormat = new DecimalFormat("0.00");

        try {
            // set-up driver for database connection
            Class.forName("sun.jdbc.odbc.JdbcOdbcDriver");

            // identifies Microsoft Access database file
            System.out.println("Design, " + "Class I, " +
                    "Class II, " + "Class III, " + "Class IV, " +
             "ERMP");
            for (int fileNumber = 1; fileNumber<258; fileNumber++) {
                String filename = "C:/Documents and Settings/" +
                        "Christopher Nannini/Desktop/ +
                        OPTINT DATA COMPLETE/" +
                        "ASCU" + Integer.toString(fileNumber) + ".mdb";
                String database = "jdbc:odbc:Driver={Microsoft Access +
                        Driver(*.mdb)};DBQ=";
                database+= filename.trim()+
                        ";DriverID=22;READONLY=true}";

                // creates a connection to the database
                Connection con = DriverManager.getConnection(
```

```java
                        database ,"","");

                // creates a java.sql.Statement to run queries
                Statement s = con.createStatement();
                double totalOpenTime = 0.0;
                double totalCoveredTime = 0.0;
                double percentCovered = 0.0;
                String[] platform = {"Class I", "Class II",
                "Class III", "Class IV", "ERMP"};
                System.out.print("ASCU" +
                        Integer.toString(fileNumber));
                for (int i = 0; i<5; i++) {

                    // build Strings to interact with the database
                    String columns = "Mission, MissionPlatformType, " +
                            "openTime, coveredTime ";
                    String table = " FROM CoverageByType ";
                    String filter = " WHERE MissionPlatformType='" +
                            platform[i] + "'";
                    String query = "SELECT " + columns + table +
                            filter;
                    ResultSet rs = s.executeQuery(query);

                    // iterates through the ResultSet and calculates
                       totals
                    while (rs.next()) {
                        String openTime = rs.getString("openTime");
                        String coveredTime =
                                rs.getString("coveredTime");

                        totalOpenTime = totalOpenTime +
                                Double.parseDouble(openTime);
                        totalCoveredTime = totalCoveredTime +
                                Double.parseDouble(coveredTime);
                    }
                    if (totalOpenTime == 0) {
                        System.out.print(", ");
                        System.out.print("0.00");
                    }
                    else {
                        System.out.print(", ");
                        System.out.print(numberFormat.format(
                                100*(totalCoveredTime/totalOpenTime)));
                    }
                }
                // close statement and connection to database
                s.close();
                con.close();
                System.out.println("");
            }
        } catch (Exception err) {
            System.out.println("ERROR: " + err);
        }
    }
}
```

LIST OF REFERENCES

AAI Corp. awarded contract by Honeywell for 55 micro UAV prototype airframes. (2006). Retrieved April 11, 2006 from http://www.shephard.co.uk/UVOnline/Default.aspx?Action=-187126550&ID=8511352c-ef37-45eb-a558-c9f129387529

Army orders ground control station for Warrior UAV. (2005). Retrieved April 24, 2006 from http://mae.pennnet.com/Articles/Article_Display.cfm?ARTICLE_ID=238154&p=32

Ducted fan miniature unmanned air vehicle. (2005). Retrieved April 11, 2006 from http://www.defense-update.com/products/h/honeywell-mav.htm

ERMP extended-range multi-purpose UAV. (2005). Retrieved April 5, 2006 from http://www.defense-update.com/products/e/ermpUAV.htm

FCS dismounted controller device (DCD) background summary. (2005). Retrieved April 25, 2006 from http://www.boeing.com/defense-space/ic/fcs/bia/050420_dcd_summary.html

Fire scout UAV officially joins U.S. army. (2004). Retrieved April 19, 2006 from http://cndyorks.gn.apc.org/yspace/articles/firescout3.htm

Four FCS UAV sub-contracts awarded (updated). (2005). Retrieved April 10, 2006 from http://www.defenseindustrydaily.com/2005/10/four-fcs-uav-subcontracts-awarded-updated/index.php

One small step for a UAV, one big step for FCS Class I. (2005). Retrieved April 11, 2006 from http://www.defenseindustrydaily.com/2005/10/one-small-step-for-a-uav-one-big-step-for-fcs-class-i/index.php

Organic air vehicle (OAV). (2005). Retrieved April 5, 2006 from http://www.defense-update.com/features/du-2-04/mav-oav.htm

Raven UAVs winning gold in Afghanistan's "commando olympics". (2005). Retrieved April 5, 2006 from http://www.defenseindustrydaily.com/2005/11/raven-uavs-winning-gold-in-afghanistans-commando-olympics/index.php

Unmanned aerial vehicles (UAVs). (2004, October). [Electronic version]. *Army, 54*(10) 286-288. Retrieved April 11, 2006, from ProQuest database.

Unmanned aircraft system roadmap 2005-2030. (2005). Unpublished manuscript. Retrieved April 10, 2006, from www.acq.osd.mil/usd/Roadmap%20Final2.pdf

U.S. Army extends AAI's TUAV system contract after successful operational test. (2001). Retrieved April 10, 2006 from http://www.aaicorp.com/corporate/press/tuavextend.html

106th Congress (2000). National Defense Authorization, Fiscal Year 2001, Sec 220.

Ahner, D. M. (2005a). *Description of assignment scheduling capability for UAVs (ASC-U) simulation tool and UAV mix formulation.* TRAC-Monterey, Monterey, CA:

Ahner, D. M. (2005b). *UAV mix screening tool.* TRAC-Monterey, Monterey, CA: Briefing Slides.

Ahner, D. M., Buss, A. H., & Ruck, J. (2006). *ASC-U users/analyst manual.* Unpublished manuscript.

Bone, E., & Bolkcom, C. (2003). *Unmanned aerial vehicles: background issues for congress* (RL31872) Congressional Research Service. Retrieved April 10, 2006, from www.fas.org/irp/crs/RL31872.pdf

Brown, L. P. (2000). *Agent based simulation as an exploratory tool in the study of the human dimension of combat.* Master's Thesis, Naval Postgraduate School, Monterey, California.

Buss, A. H. (2006). Simkit. Retrieved June 6, 2006 from http://diana.gl.nps.navy.mil/Simkit/

Cioppa, T. M. (2002). *Efficient nearly orthogonal and space-filling experimental designs for high-dimensional complex models.* Doctoral Dissertation, Naval Postgraduate School, Monterey, California.

Crane, D. (2005). *Micro air vehicle: Backpackable UAV for tactical reconnaissance & surveillance.* Retrieved April 11, 2006 from http://www.defensereview.com/modules.php?name=News&file=article&sid=811

Devore, J. L. (2004). *Probability and statistics for engineering and the sciences* (6th ed.). Belmont, CA: Brooks/Cole - Thomson Learning.

Erwin, S. I. (2003). Army to field four classes of UAVs. *National Defense, 87*(593), 33.

Farmer, M. P. (2001). *Feasibility of the tactical UAV as a combat identification tool.* Master's Thesis, Naval Postgraduate School, Monterey, California.

Goebel, G. (2006). *Modern U.S. endurance UAVs.* Retrieved April 10, 2006 from http://www.vectorsite.net/twuav_13.html

Hakola, M. B. (2004). *An exploratory analysis of convoy protection using agent-based simulation.* Master's Thesis, Naval Postgraduate School, Monterey, California.

Havens, M. E. (2002). *Dynamic allocation of fires and sensors.* Master's Thesis, Naval Postgraduate School, Monterey, California.

Henry, C. M. (2002). Drug development. *Chemical & Engineering News, 80*(22) 53-66.

Jenkins, G. E., & Snodgrass, W. J. Jr. (2005). *The Raven small unmanned aerial vehicle (SUAV), investigating potential dichotomies between doctrine and practice.* MBA Professional Report, Naval Postgraduate School, Monterey, California.

John, D. G., Shaver, R., Lynch, K. F., Amouzegar, M. A., & Snyder, D. (2005). *Unmanned aerial vehicle end-to-end support considerations* (MG-350). Santa Monica, CA: RAND Corporation. Retrieved April 10, 2006, from http://www.rand.org/pubs/monographs/MG350/index.html

Kelton, W. D. (2001). Some modest proposals for simulation software: design and analysis of experiments. *34th Annual Simulation Symposium, SS01* 0237.

Kleijnen, J. P. C. (2004). Design and analysis of Monte Carlo experiments. In J. E. Gentle, W. Haerdle & Y. Mori (Eds.), *Handbook of computational statistics: concepts and fundamentals* (1st ed.). New York: Springer-Verlag.

Kleijnen, J. P. C., Sanchez, S. M., Lucas, T. W., & Cioppa, T. M. (2005). State-of-the-art review. A user's guide to the brave new world of designing simulation experiments *INFORMS Journal on Computing, 17*(3), 263-289.

Knarr, W. M., Haskins, S., & Mouras, T. P. (2001). Army transformation and the tactical unmanned aerial vehicle (TUAV) system. [Electronic version]. *Military Intelligence Professional Bulletin, 27*(2), 50. Retrieved June 12, 2006, from ProQuest database.

Latimer, J. C. (2005). *Prospector UAS.* Retrieved April 5, 2006 from http://www.tbe.com/products/uav/prospector.asp

Mahnken, C. (2002). *Army's shadow tactical unmanned aerial vehicle to begin full rate production.* Retrieved April 10, 2006 from https://uav.peoavn.army.mil/UAVWN%20Shadow%20Full.HTM

Montgomery, D. C., Peck, E. A., & Vining, G. G. (2001). *Introduction to linear regression analysis* (3rd ed.). New York, NY: John Wiley & Sons, Inc.

Sall, J., Creighton, L., & Lehman, A. (2005). *JMP start statistics: a guide to statistics and data analysis using JMP and JMP IN software* (3rd ed.). Belmont, CA: Brooks/Cole - Thomson Learning.

Sanchez, S. M. (2005). Nearly Orthogonal Latin Hypercube Design Excel® Spreadsheet. Retrieved June 6, 2006 from http://diana.cs.nps.navy.mil/seedlab/

Sinclair, E. J. Brigadier General. (2005). *2005 UAVS Symposium*. Briefing Slides. Retrieved June 6, 2006 from www.quad-a.org/Symposiums/UAV-05/Presentations/

Tabachnick, B. G., & Fidell, L. S. (1989). *Using multivariate statistics* (2nd ed.). New York, NY: Harper & Row.

Witsken, J. C. (2004). *Army UAV mix analysis study plan* (Draft 1.3) TRADOC Analysis Center, 255 Sedgwick Avenue, Ft. Leavenworth, Kansas 66027.

Wolf, E. (2003). *Using agent-based distillations to explore logistics support to urban, humanitarian assistance/disaster relief operations.* Master's Thesis, Naval Postgraduate School, Monterey, California.

INITIAL DISTRIBUTION LIST

1. Defense Technical Information Center
   Ft. Belvoir, Virginia

2. Dudley Knox Library
   Naval Postgraduate School
   Monterey, California

3. Professor Arnold H. Buss
   Modeling, Virtual Environments, and Simulation Institute
   Naval Postgraduate School
   Monterey, California

4. Professor Susan M. Sanchez
   Department of Operations Research
   Naval Postgraduate School
   Monterey, California

5. Major Darryl K. Ahner
   TRAC-MTRY
   Monterey, California

6. LTC Jeffrey Schamburg
   TRAC-MTRY
   Monterey, California

7. TRADOC Analysis Center
   ATTN ATRC (Mr. Bauman)
   Fort Leavenworth, Kansas

8. Director
   Marine Corps Research Center, Code C40RC
   Marine Corps Combat Development Command (MCCDC)
   Quantico, Virginia

9. Major Christopher J. Nannini
   Naval Postgraduate School
   Monterey, California